CHAPTER IV
RESULTS AND DISCUSSION

In this work, different Si/Al_2 ratio zeolites including 2.0, 2.5 and 5 Si/Al_2 ratios designated by 2.0X, 2.5X and Y, respectively, were used to investigate zeolite acidity effects on the xylene separation. In addition, the zeolite was exchanged with di-valent series cations, *Ba, Sr, Ca* and *Mg*, for further investigation on the effect of acidity.

Here, the zeolite acidity is respresented by S_{int}, the intermediate electronegativity, as calculated by equation (2.5). The higher the S_{int}, the higher the acidity. From equation (2.5), zeolite acidity depends on the electronegetivity of an exchanged metal cation, Si, Al and O (S_M, S_{Si}, S_{Al}, S_O) and a number of each atom in a unit cell (p, q, r, t). Thus, zeolite acidity can be adjusted by changing atoms in zeolite and/or number of atoms in one unit cell. By varying the exchangeable cation, the zeolite acidity can be adjusted. For the same Si/Al_2 ratio, zeolite acidity increases from *Ba, Sr, Ca* and *Mg* exchanged zeolite which corresponds to the decrease in the cationic size from *Ba, Sr, Ca* and *Mg*. By varying the Si/Al_2 ratio, a number of atoms in a unit cell are changed, which, in turn, affects zeolite acidity. Zeolite acidity increases with the increasing of Si/Al_2 ratio from 2.0, 2.5 and 5.

4.1 Pulse Test Technique Results

Concentrations of *p*-xylene, *m*-xylene, *o*-xylene and ethylbenzene eluted from the adsorption column packed with different zeolites are shown in Figures 4.1-4.12. n-C_9 was used as a tracer or reference component because it is not adsorbed in the zeolite pore. Therefore, retention volume of the tracer corresponds to the void volume in the column. By using the ratio of the net retention volume of *p*-xylene to the net retention volume of other C_8 aromatics, *p*-xylene selectivity with respect to other components were calculated. The results are shown in Tables 4.1, 4.2 and 4.3.

Table 4.1 *p*-xylene selectivity calculated from the Pulse Test experiments with respect to the other components of *2.0X* zeolites

2.0X zeolites	*p*-xylene/ethylbenzene	*p*-xylene/*o*-xylene	*p*-xylene/*m*-xylene
Mg2.0X	0.985	1.030	0.778
Ca2.0X	1.189	0.721	0.693
Sr2.0X	1.37	0.607	0.683
Ba2.0X	2.117	2.261	2.436

Table 4.2 *p*-xylene selectivity calculated from the Pulse Test experiments with respect to the other components of *2.5X* zeolites

2.5X zeolites	*p*-xylene/ethylbenzene	*p*-xylene/*o*-xylene	*p*-xylene/*m*-xylene
Mg2.5X	1.228	0.866	0.909
Ca2.5X	1.512	0.612	0.652
Sr2.5X	2.138	0.904	0.674
Ba2.5X	2.326	1.994	2.249

Table 4.3 *p*-xylene selectivity calculated from the Pulse Test experiments with respect to the other components of *Y* zeolites

Y zeolites	*p*-xylene/ethylbenzene	*p*-xylene/*o*-xylene	*p*-xylene/*m*-xylene
MgY	1.190	0.891	1.026
CaY	1.335	0.694	0.822
SrY	1.444	0.840	0.983
BaY	1.707	1.257	1.488

As expected, with larger exchanged-cation, Ba^{2+}, *p*-xylene selectivity with respect to the other C_8 aromatics increases. The reason is that Ba^{2+} exchanged zeolite posses low acidity and *p*-xylene is the least basic species among the C_8 aromatics; therefore, *Ba2.0X, Ba2.5X*, and *BaY* have higher *p*-xylene selectivity than

their corresponding zeolite exchanged with the other cations. Because zeolite acidity increases with Si/Al_2, one would expect that *2.0X* would have the highest *p*-xylene selectivity. The trend is not so except p-xylene selectivity with respect to *m*-xylene as well as *o*-xylene and ethylbenzene. To elucidate this unusual behavior, the selectivity is plotted along with the cationic radius and S_{int} as shown in Figures 4.13-4.15.

As shown in Figures 4.13-4.14, both zeolite acidity and exchanged-cation size affect *p*-xylene selectivity. The *p*-xylene selectivity with respect to *o*-xylene and *m*-xylene dramatically decreases from *Ba* to *Sr* because the effect of acid-base interaction. That is a low basic xylene prefers to adsorb on low acid zeolite. As the aromatic π basicity of xylenes decreases from *m*-xylene, *o*-xylene, *p*-xylene to ethylbenzene (Bathomeuf, 1996). *p*-xylene tends to adsorb less on high acid zeolite. In other words, the selectivity of *p*-xylene with respect to the other species decreases with the increasing of zeolite acidity. However, from *Sr* to *Mg*, the *p*-xylene selectivity with respect to *o*-xylene and *m*-xylene is not significantly affected by the zeolite acidity but the exchanged cation size. So, if an exchanged cation is big enough to occupy the space in the supercage, which, in turn, hinders the adsorption of *p*-xylene, the selectivity of *p*-xylene is dictated by the cation size. *p*-xylene selectivity with respect to ethylbenzene is different from that with respect to *o*-xylene and *m*-xylene. The selectivity decreases from *Ba* to *Mg*. It is clear that only acid-base interaction governs the selectivity.

The result on Y zeolite is shown in Figure 4.15. For *Y* zeolite, the trends of *p*-xylene selectivity with respect to the other species are the same as that on *2.0X* and *2.5X* zeolite. However, there is a big different in the magnitude. *p*-xylene selectivity with respect to *o*-xylene and *m*-xylene does not significantly decrease from *Ba* to *Sr* as in the 2.0X and 2.5X zeolite. That may be because the *p*-xylene selectivity is not mainly governed by the zeolite acidity. Since Y zeolite acidity is relatively high, acidity of BaY is significant enough to prevent *p*-xylene adsorb on the zeolite. So, when the zeolite acidity increases from *BaY* to *SrY* , only a small change in the *p*-xylene selectivity is observed. From *Sr* to *Mg* exchanged zeolite, *p*-xylene selectivity with respect to *o*-xylene and *m*-xylene is likely affected by the cation size than the zeolite acidity, as the selectivity is relatively constant with the change of the

acidity. *p*-xylene selectivity with respect to ethylbenzene has the same behavior as in the case of *2.0X* and *2.5X* zeolite.

4.2 Breakthrough Technique Results

The same adsorbents as in the Pulse Test experiments were used for the Breakthrough experiments. Figures 4.16 - 4.27 show results from the experiments. The plots can be interpreted in the same way as in the Pulse Test experiments. *p*-xylene selectivity with respect to the other components of *2.0X*, *2.5X* and *Y* zeolite are shown in Tables 4.4-4.6. Again, the same trend as in the Pulse Test results on how *p*-xylene selectivity is affected by the cationic size and Si/Al_2 ratio are obtained.

Figure 4.28 shows *p*-xylene selectivity on 2.0X zeolite. From *Ba* to *Sr*, *p*-xylene selectivity is controlled by the effect of the acid-base interaction. However, from *Sr* to *Mg*, *p*-xylene selectivity with respect to *o*-xylene and *m*-xylene seems to be controlled by the effect of cation size as can be seen that the selectivity slightly increases from *Sr* to *Mg*. *p*-xylene selectivity with respect to ethylbenzene keeps going down but not significantly. So, the *p*-xylene selectivity with respect to ethylbenzene is probably controlled by the effect of acid-base interaction for all di-valence series cation exchanged 2.0X zeolites.

Pulse Test results on *2.5X* zeolite are shown in Figure 4.29. Two trends are observed. First, *p*-xylene selectivity with respect to ethylbenzene continuously decreases from *Ba* to *Mg* because of the effect of acid-base interaction. The second trend is *p*-xylene selectivity with respect to *o*-xylene and *m*-xylene, dramatically decreases from *Ba* to *Sr* because the effect of the acid-base interaction mainly governs the *p*-xylene selectivity. However, from *Sr* to *Ca*, the effect of the acid-base interaction may not play a significant role because only a slight decrease in the *p*-xylene selectivity can be observed. From *Ca* to *Mg*, the effect of cation size starts to control the *p*-xylene selectivity as seen from a small increase in the selectivity.

Figure 4.30 shows results on *Y* zeolite. Acidity of the *Y* zeolite is relatively high compared to *2.0X* and *2.5X* zeolite. *p*-xylene, which is a low basic xylene, does not prefer to adsorb on such the high acid zeolite. So, the *p*-xylene selectivity with respect to *o*-xylene, *m*-xylene and ethylbenzene on the *Y* zeolite are lower than both

X zeolite. From *BaY* to *SrY*, a decrease in the *p*-xylene selectivity with respect to *o*-xylene and *m*-xylene is not so significant as in the *2.0X* and *2.5X* zeolite. Because the *Y* zeolite acidity is so high that the effect of the acidity is not clearly seen. From *SrY* to *MgY*, the *p*-xylene selectivity with respect to *o*-xylene and *m*-xylene on the *Y* zeolite shows the same trend as in the *X* zeolite and can be interpreted in the same way. The *p*-xylene selectivity with respect to ethylbenzene slightly decreases from *BaY* to *MgY*. The effect of the acid-base interaction does not play a significant role on the *p*-xylene selectivity.

Results in Figures 4.13 – 4.15 and 4.28 – 4.30 show that *p*-xylene selectivity with respect to ethylbenzene are higher than one. Since the acidity of di-valence cation exchanged 2.0*X*, 2.5*X* and *Y* zeolites are high, all zeolite prefer to adsorb xylene with high basicity. And ethylbezene is the lowest basic species among its isomer, resulting in the low selectivity of ethylbenzene and high *p*-xylene selectivity.

4.3 Comparison between Pulse Test and Breakthrough Technique Results

Unlike in the real applications, in the Pulse Test study, concentration of the feed is low because only 2 ml of the feed is injected into the column and is diluted by the desorbent stream, which is toluene. The Breaktrough Test, however, involves a high concentration study without any dilution of desorbent stream. As a result, it is suggested that the Breakthrough experiments should represent what happens in real applications better than the Pulse Test experiments. Figures 4.31-4.33 show the comparison of *p*-xylene selectivity calculated from the Breakthrough and Pulse Test experiments on *2.0X*, *2.5X* and *Y* zeolite, respectively. Both results show the same trend but different in the magnitude. And these two techniques show the effect of the feed concentration on the adsorbate-adsorbent interaction. For the *p*-xylene selectivity with respect to *o*-xylene and *m*-xylene, the selectivity from both results are comparable. However, for the *p*-xylene selectivity with respect to ethylbenzene, the results from these two techniques are different for *Ba*, *Sr* and *Ca* exchanged zeolite.

In previous work, mono-valence cation exchanged zeolites were studied; *KY* zeolite provided an excellent property on *p*-xylene selectivity (Suntornpun, 2002). In this work, *Ba2.5X* zeolite has the hightest *p*-xylene selectivity among the di-valence cation exchanged zeolites. Interestingly, *KY* and *Ba2.5X* are similar in the S_{int} and cationic radius. S_{int} of *KY* and *Ba2.5X* are 2.6507 and 2.6619, respectively. Cationic radius of *K* is 1.35 $Å^2$ and *Ba* is 1.33 $Å^2$. Thus, the optimum of S_{int} and cation size may be in these ranges.

Table 4.4 *p*-xylene selectivity calculated from Breakthrough experiment with respect to the other components of *2.0X* zeolites

2.0X zeolites	*p*-xylene/ethylbenzene	*p*-xylene/*o*-xylene	*p*-xylene/*m*-xylene
Mg2.0X	0.985	0.778	1.030
Ca2.0X	1.189	0.693	0.721
Sr2.0X	1.37	0.683	0.607
Ba2.0X	2.675	3.269	2.683

Table 4.5 *p*-xylene selectivity calculated from Breakthrough experiment with respect to the other components of *2.5X* zeolites

2.5X zeolites	*p*-xylene/ethylbenzene	*p*-xylene/*o*-xylene	*p*-xylene/*m*-xylene
Mg2.5X	1.192	0.946	0.909
Ca2.5X	1.513	0.469	0.487
Sr2.5X	2.3	0.878	0.699
Ba2.5X	2.614	2.745	2.854

Table 4.6 *p*-xylene selectivity calculated from Breakthrough experiment with respect to the other components of *Y* zeolites

Y zeolites	*p*-xylene/ethylbenzene	*p*-xylene/*o*-xylene	*p*-xylene/*m*-xylene
MY	1.137	1.035	1.164
CaY	1.298	0.784	0.991
SrY	1.386	0.925	1.077
BaY	1.37	1.202	1.425

4.4 Heat of Adsorption of C_8 Aromatics on *Ba2.5X*

To study the heat of adsorption of C_8 aromatics on zeolite, *Ba2.5X* was chosen. Data obtained from the Breakthrough experiment were used to calculate the heat of adsorption. According to equations (2.2) and (2.3), selectivity is a function of k_1/k_2, where k_1 and k_2 are mole fraction in solid phase and liquid phase of species 1 and 2, respectively. k_1 is a function of temperature and can be expressed as

$$k_1 = K_{01} exp\left(\frac{-\Delta H_1}{RT}\right) \tag{4.1}$$

where K_{01} is the constant of species 1, ΔH_1 is the heat of adsorption of species 1 on the adsorbent, R is the gas constant, and T is the absolute temperature. ΔH_1 and K_{01} are concentration and temperature independent parameters. Thus, selectivity can be calculated and expressed as

$$\alpha = \frac{k_1}{k_2} = \frac{K_{01}}{K_{02}} exp\left(\frac{\Delta H_2 - \Delta H_1}{RT}\right) \tag{4.2}$$

Each calculation involved a set of data at different temperature with the same adsorbed species. By using a solver function in Microsoft Excel, $\Delta H1$, K_{01}, ΔH_2 and K_{02} were calculated.

Suntornpun (2002) and Varanyanond (2001) reported the heat of adsorption of each C_8 aromatics in the presence of toluene on *KY*. Table 4.3 shows the comparison between the heat of adsorption from previous works on *KY* and this work on *Ba2.5X*.

Table 4.7 comparison between ΔH on *KY* from Varanyanond (2001), single-component adsorption and Suntornpun (2002), multi-component adsorption and the present work on *Ba2.5X*.

	ΔH on *KY* (cal/g mole)		ΔH on *Ba2.5X* (cal/g mole)
Component	Varanyanond (2001)	Suntornpun (2002)	Present work
PX	2.794	2.182	1.199
EB	1.784	1.444	0.970
OX	2.314	0.794	0.814
MX	1.784	0.732	0.842

Heat released from the adsorption of xylene would be high if xylene strongly adsorbs on the zeolite. So, the heat of adsorption would be the same trend with the adsorption order. For the multi-component system, Suntornpun's work, adsorption order on *KY* is *p*-xylene followed by ethylbenzene, *o*-xylene and *m*-xylene which corresponds to the heat of adsorption (Suntornpun, 2002). For this work, multi-component adsorption on *Ba2.5X*, the heat of adsorption shows the same trend with the adsorption order, which is *p*-xylene followed by ethylbenzene, *m*-xylene and *o*-xylene.

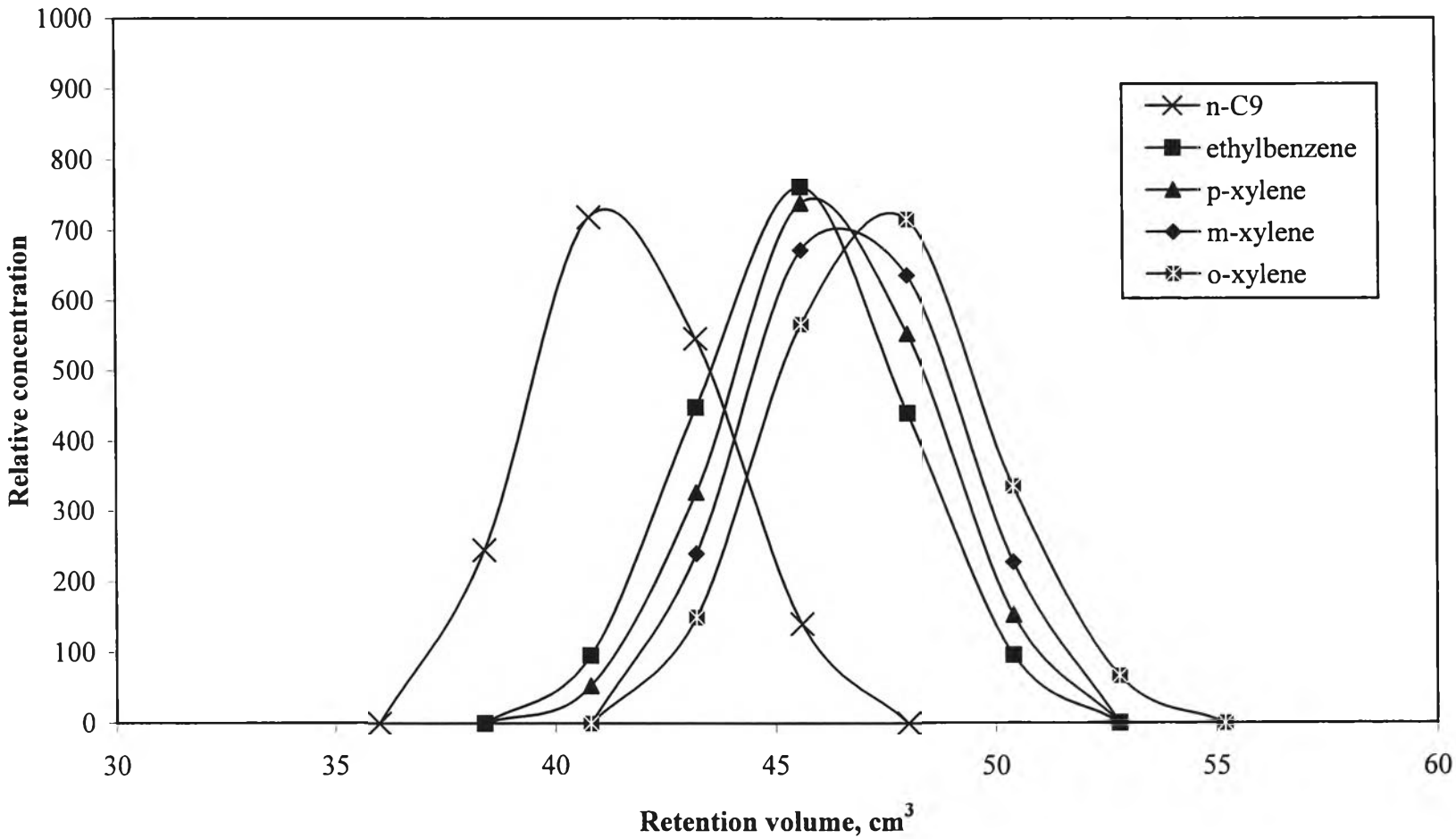

Figure 4.1 Dynamic adsorption: Multi-component pulse test on *Mg2.0X*.

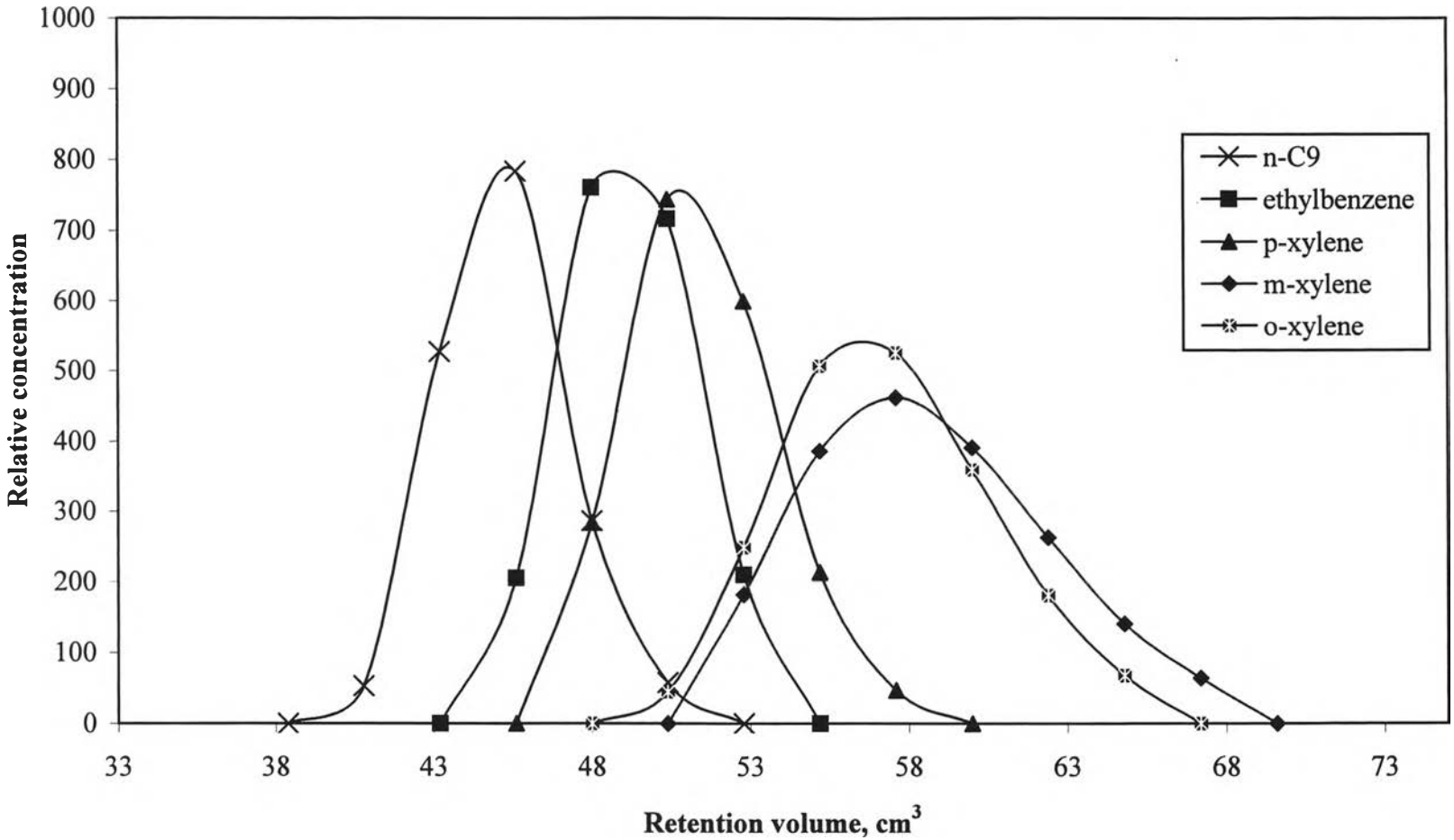

Figure 4.2 Dynamic adsorption: Multi-component pulse test on *Ca2.0X*.

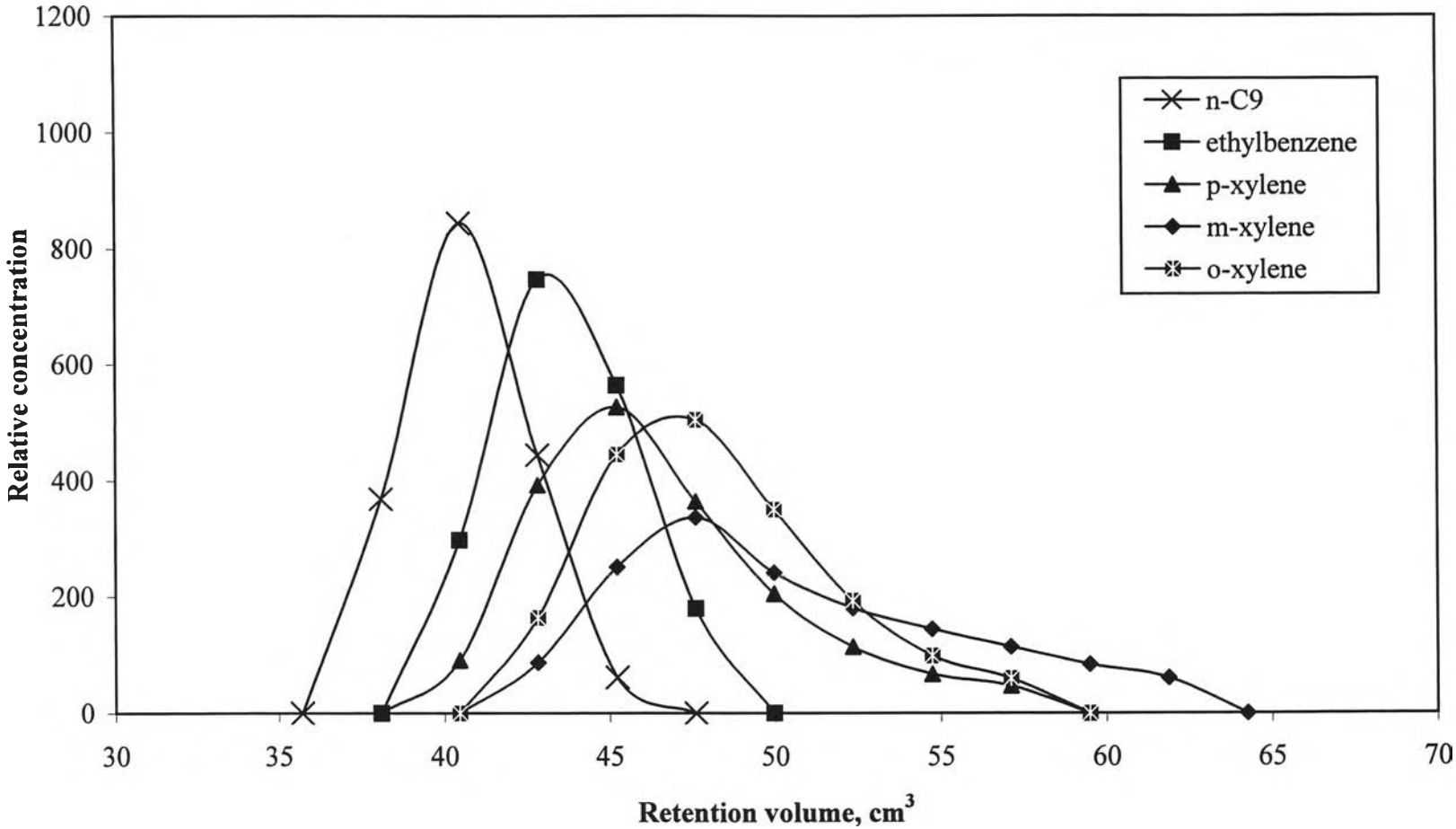

Figure 4.3 Dynamic adsorption: Multi-component pulse test on *Sr2.0X*.

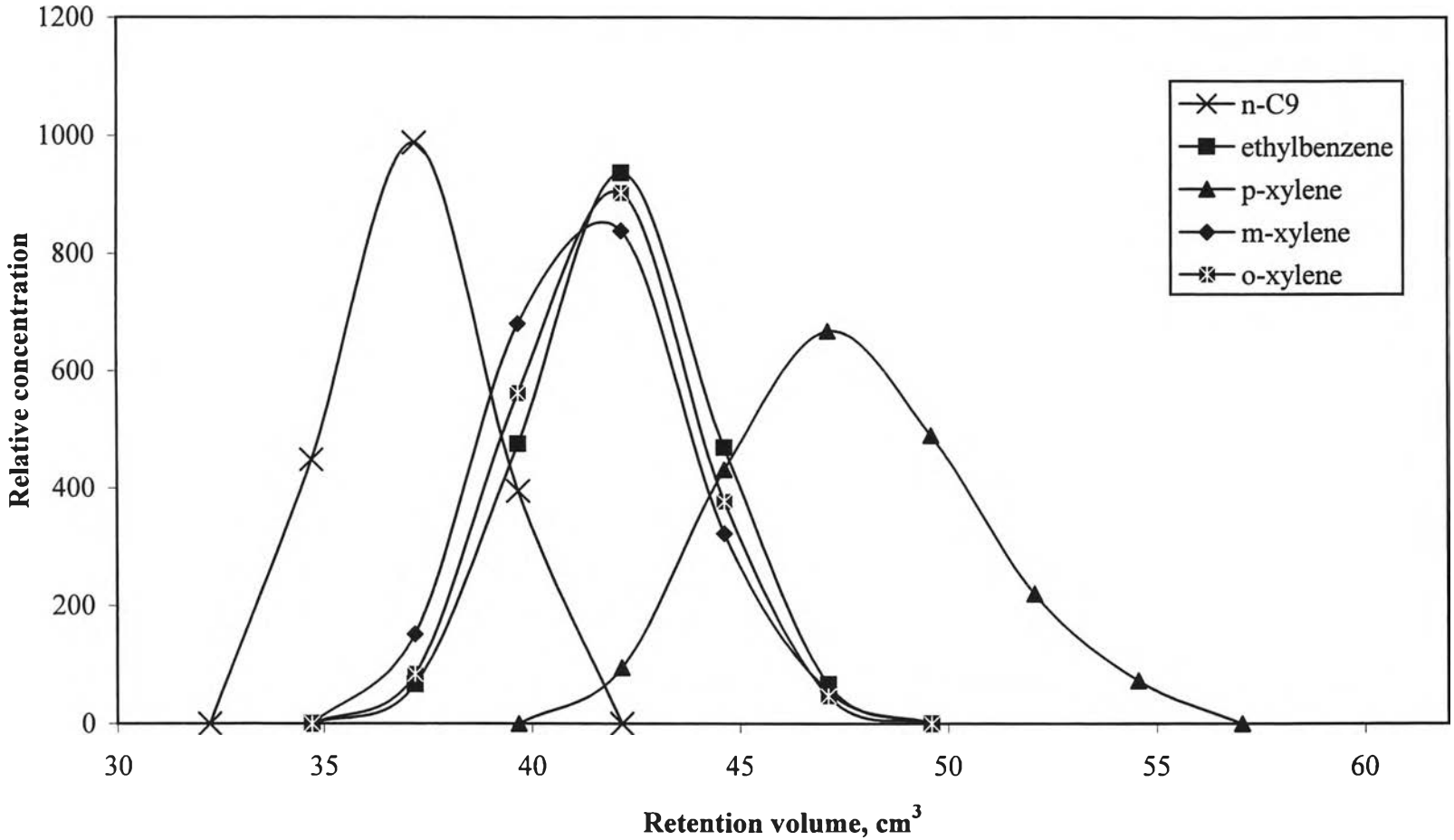

Figure 4.4 Dynamic adsorption: Multi-component pulse test on *Ba2.0X*.

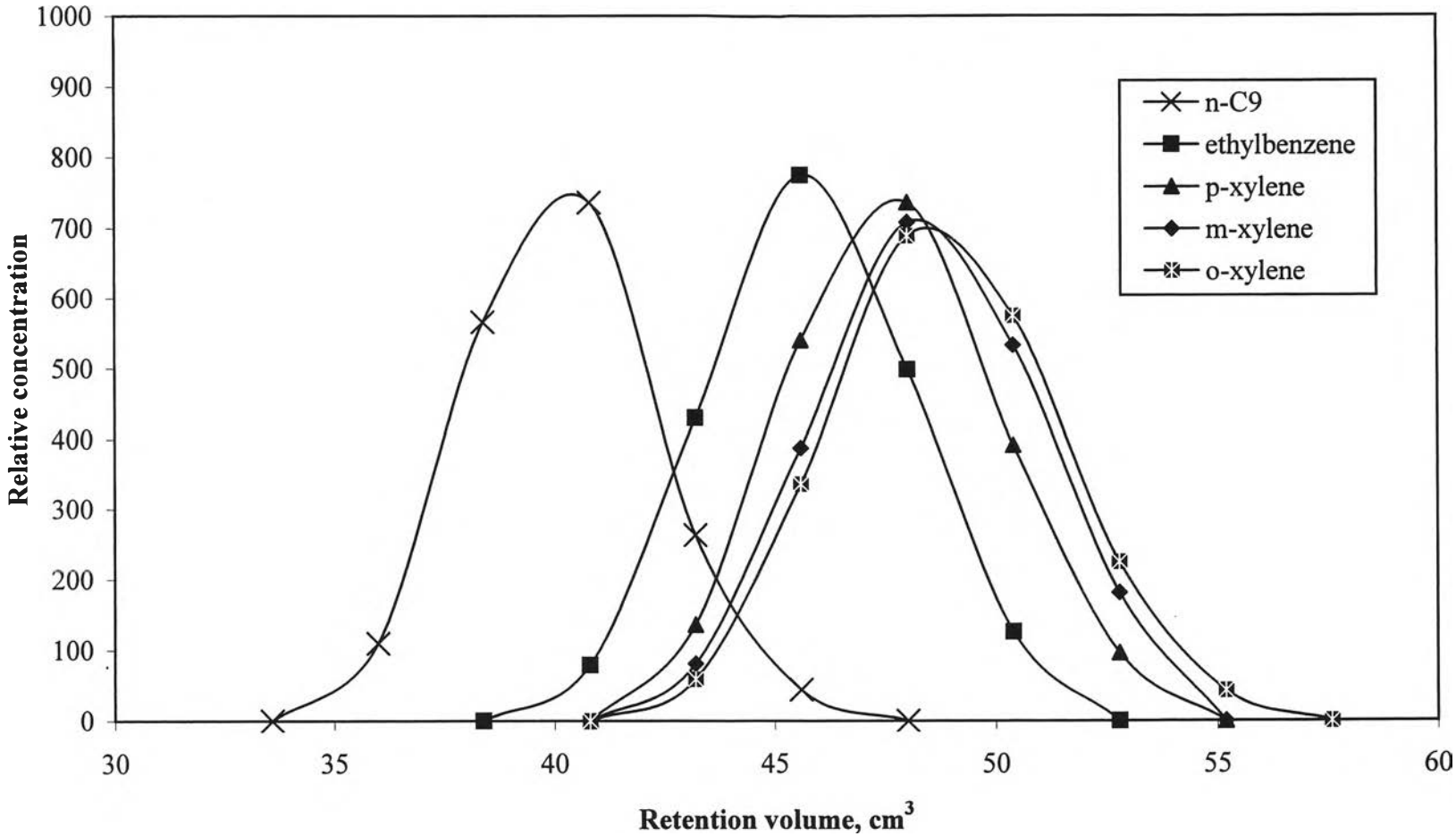

Figure 4.5 Dynamic adsorption: Multi-component pulse test on *Mg2.5X*.

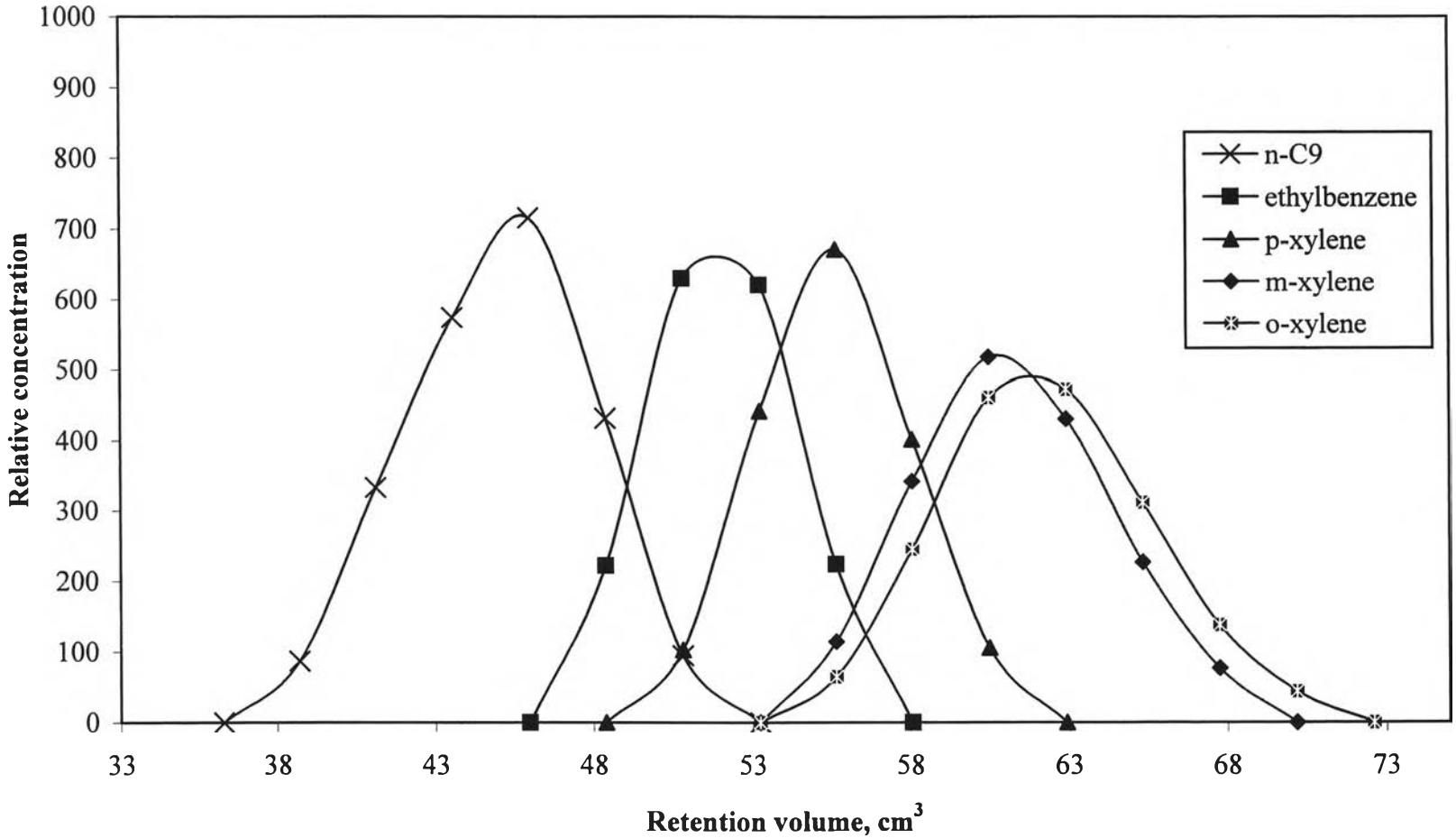

Figure 4.6 Dynamic adsorption: Multi-component pulse test on *Ca2.5X.*

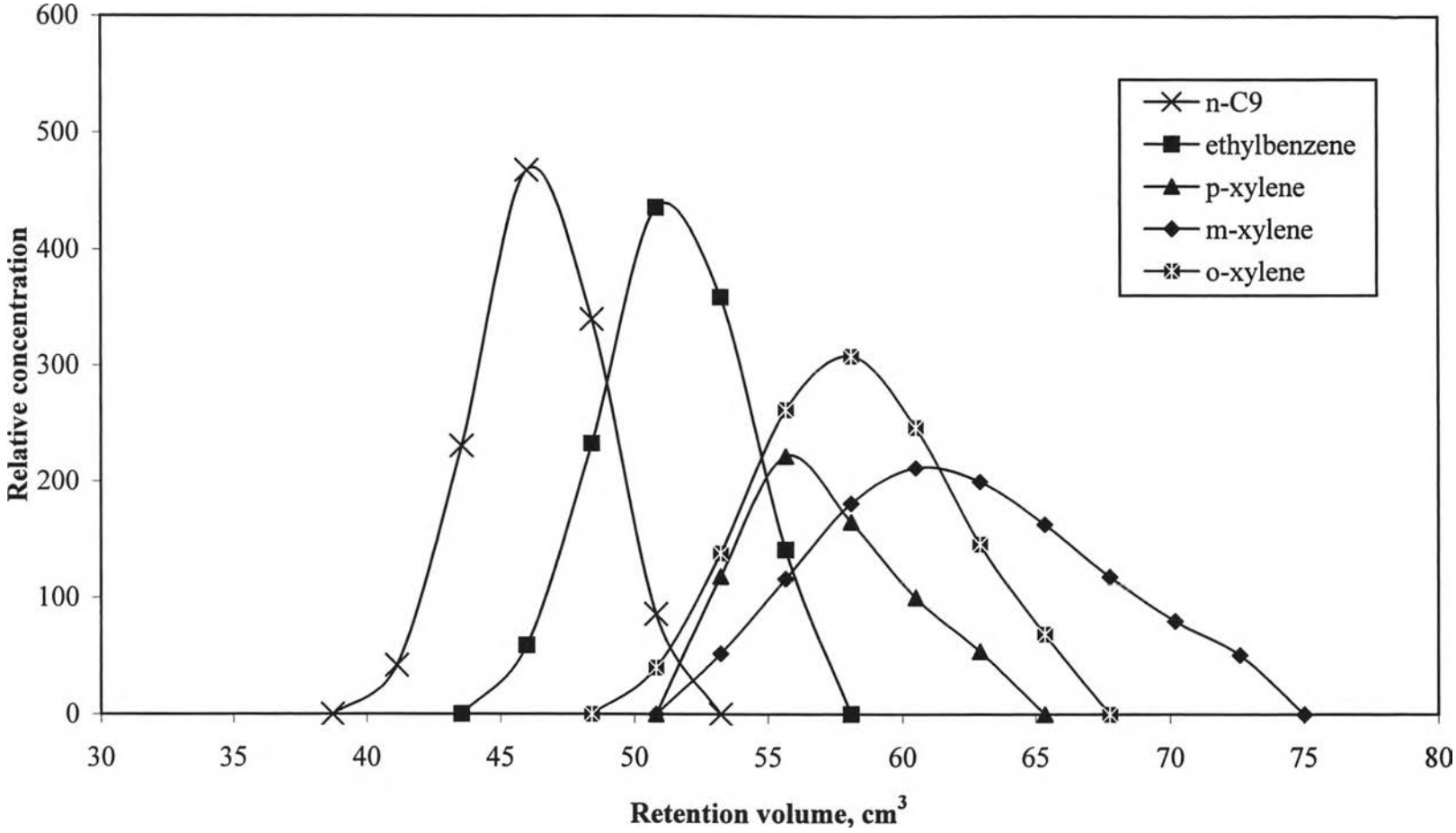

Figure 4.7 Dynamic adsorption: Multi-component pulse test on *Sr2.5X*.

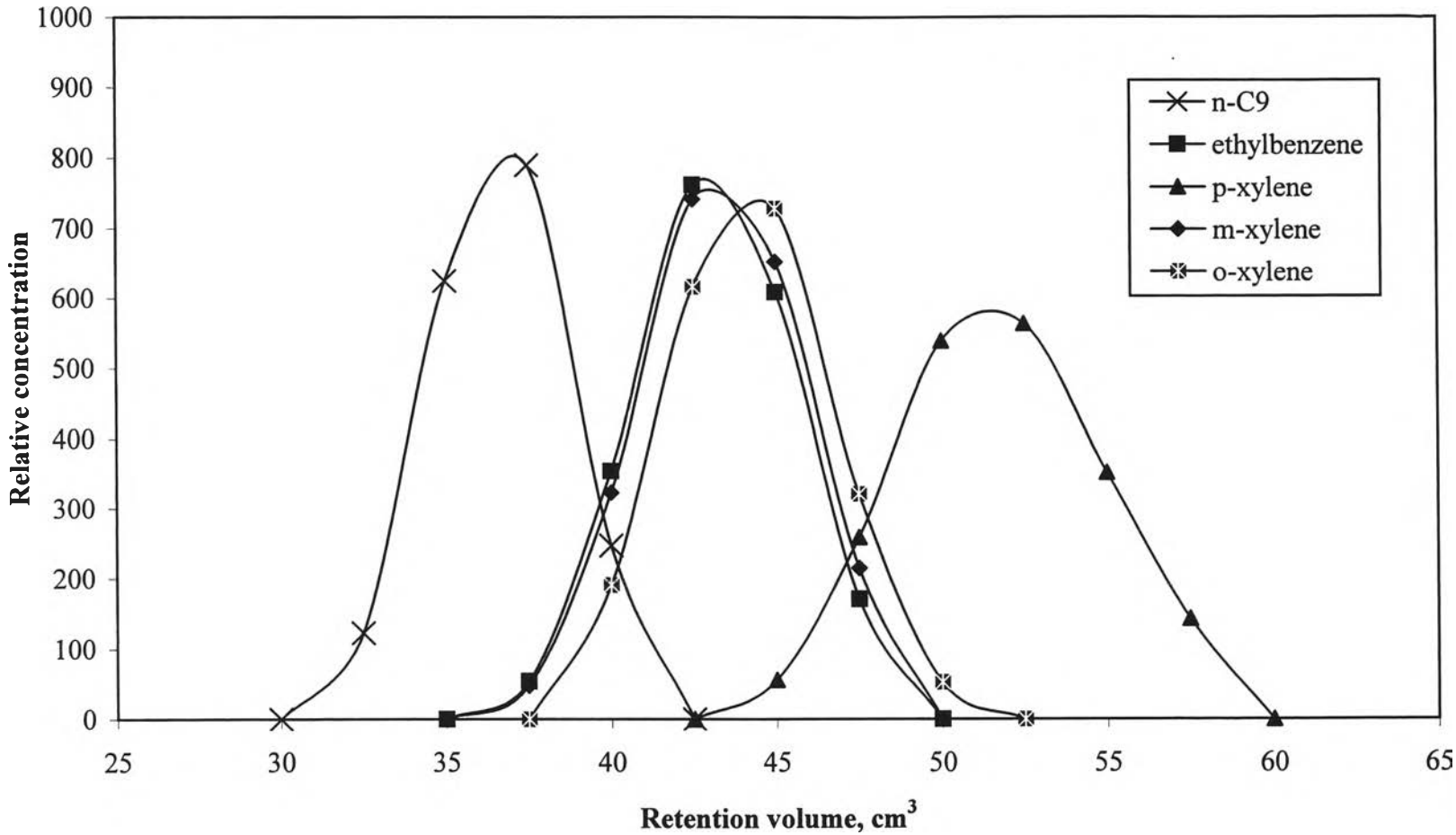

Figure 4.8 Dynamic adsorption: Multi-component pulse test on *Ba2.5X*.

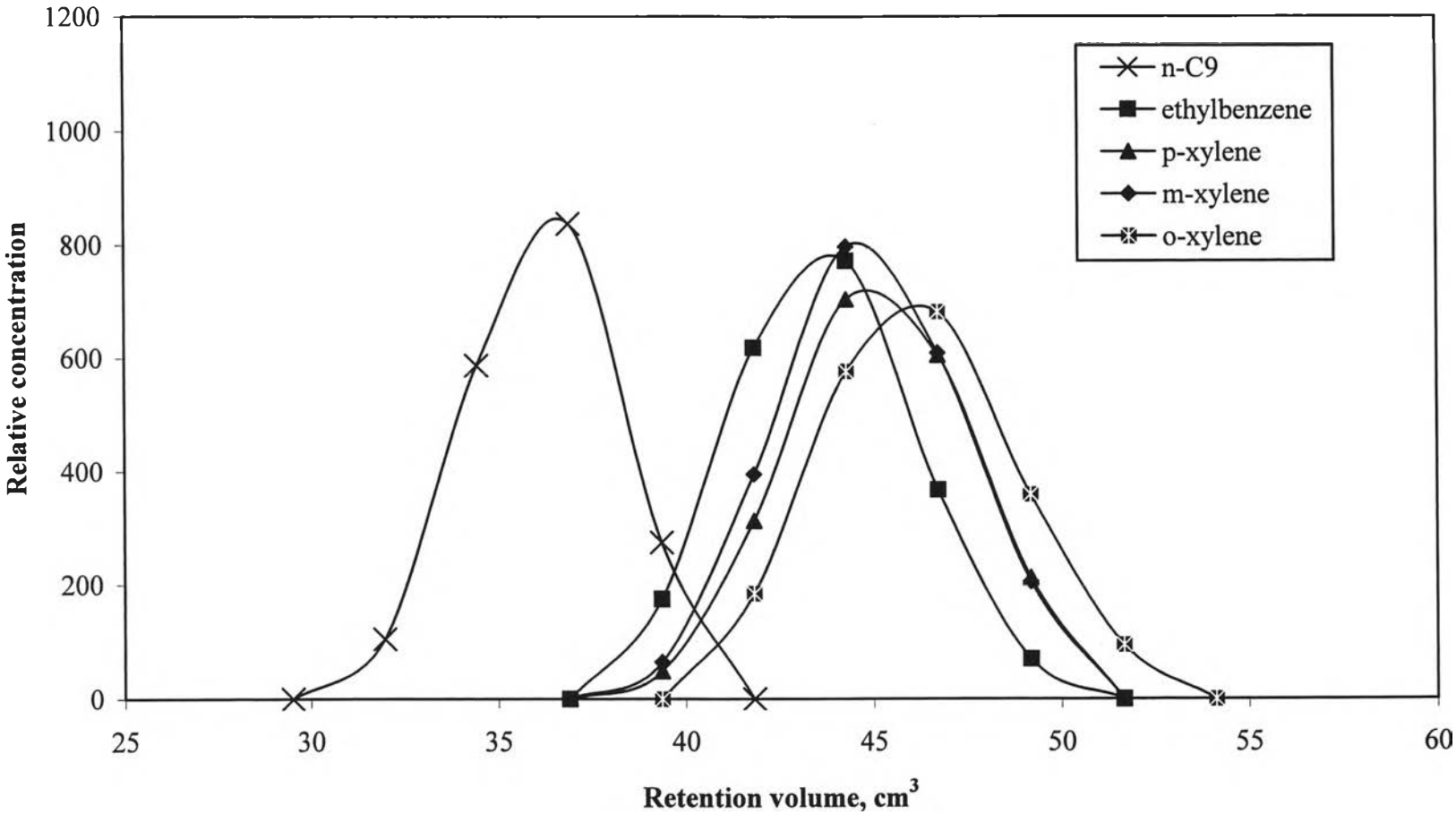

Figure 4.9 Dynamic adsorption: Multi-component pulse test on *MgY*.

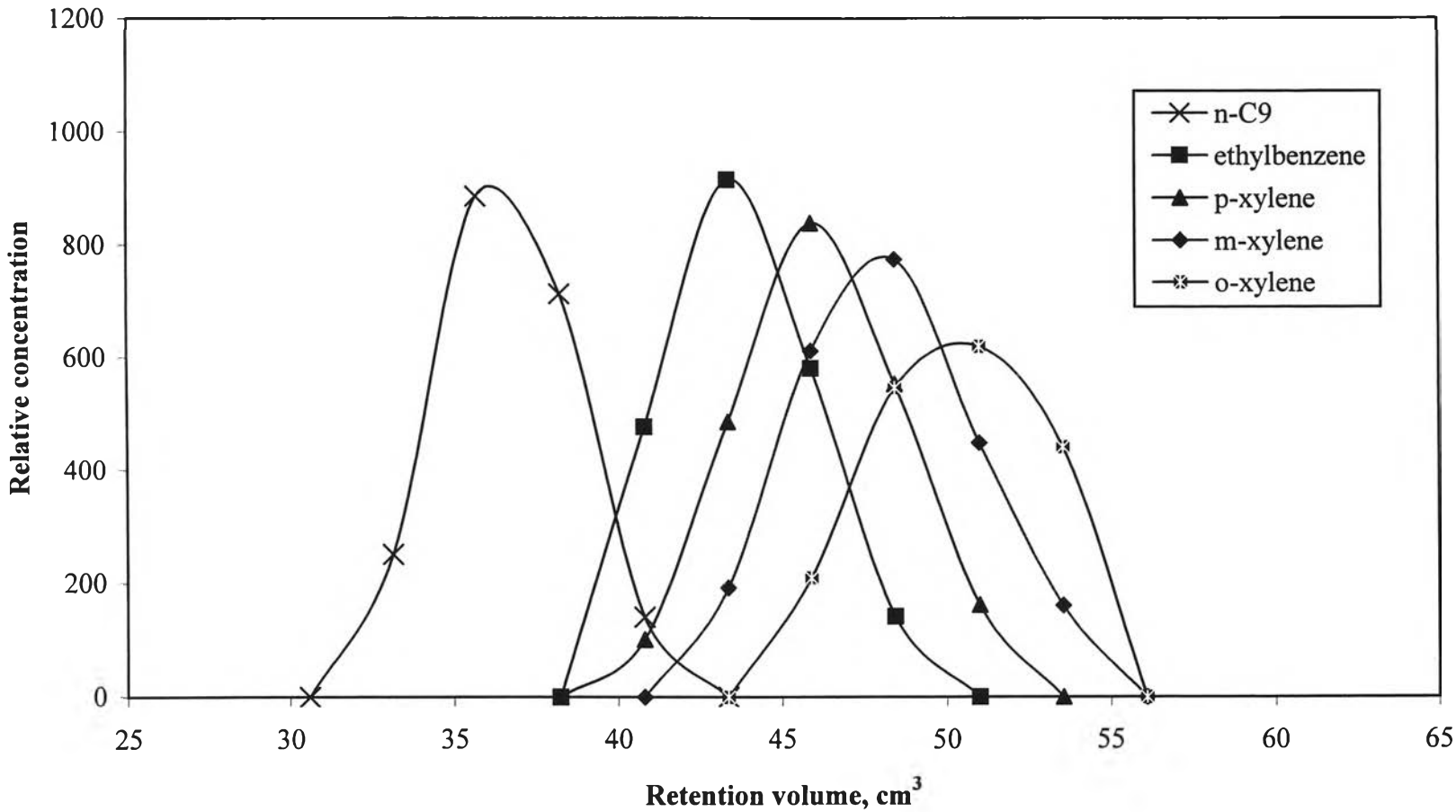

Figure 4.10 Dynamic adsorption: Multi-component pulse test on *CaY*.

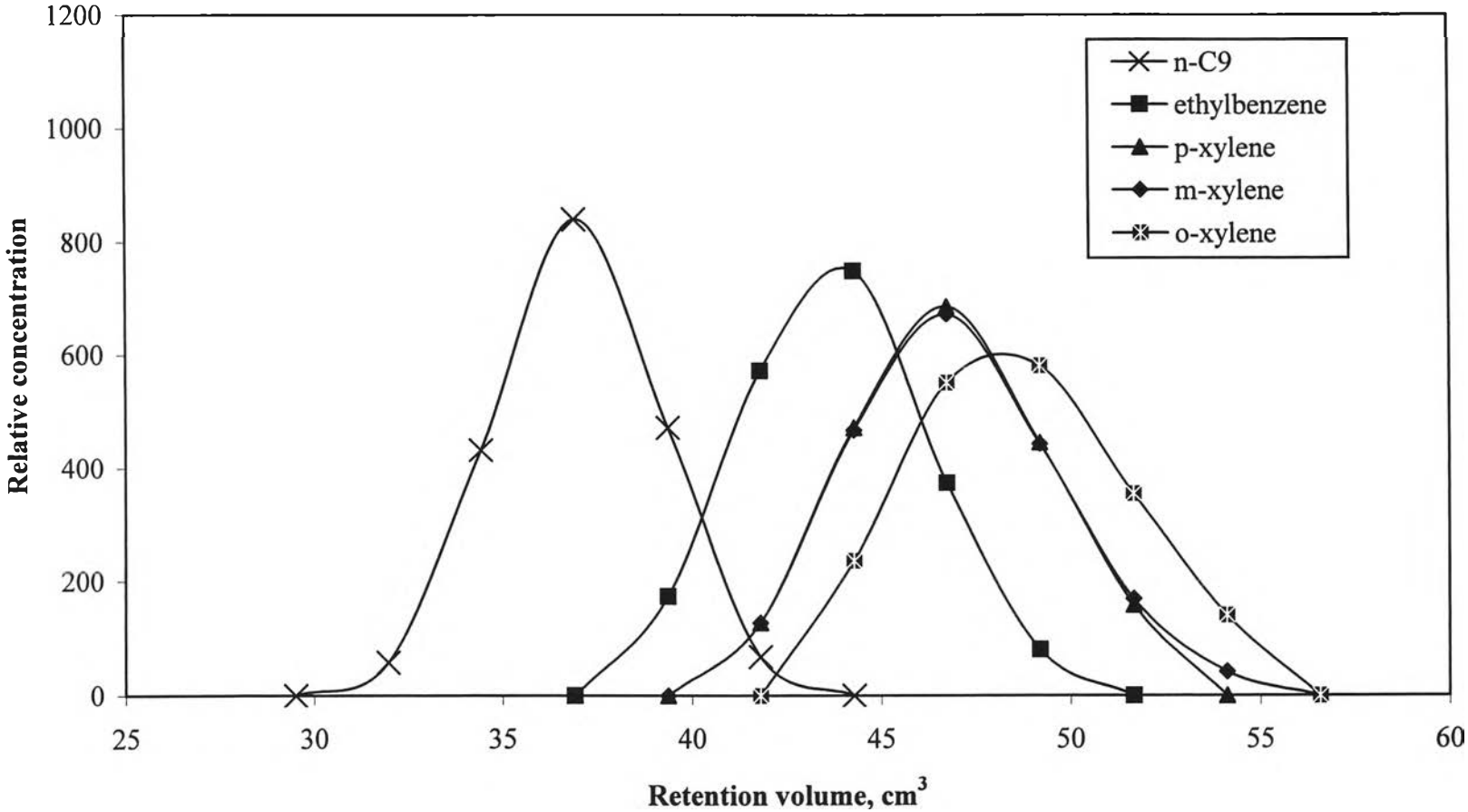

Figure 4.11 Dynamic adsorption: Multi-component pulse test on *SrY*.

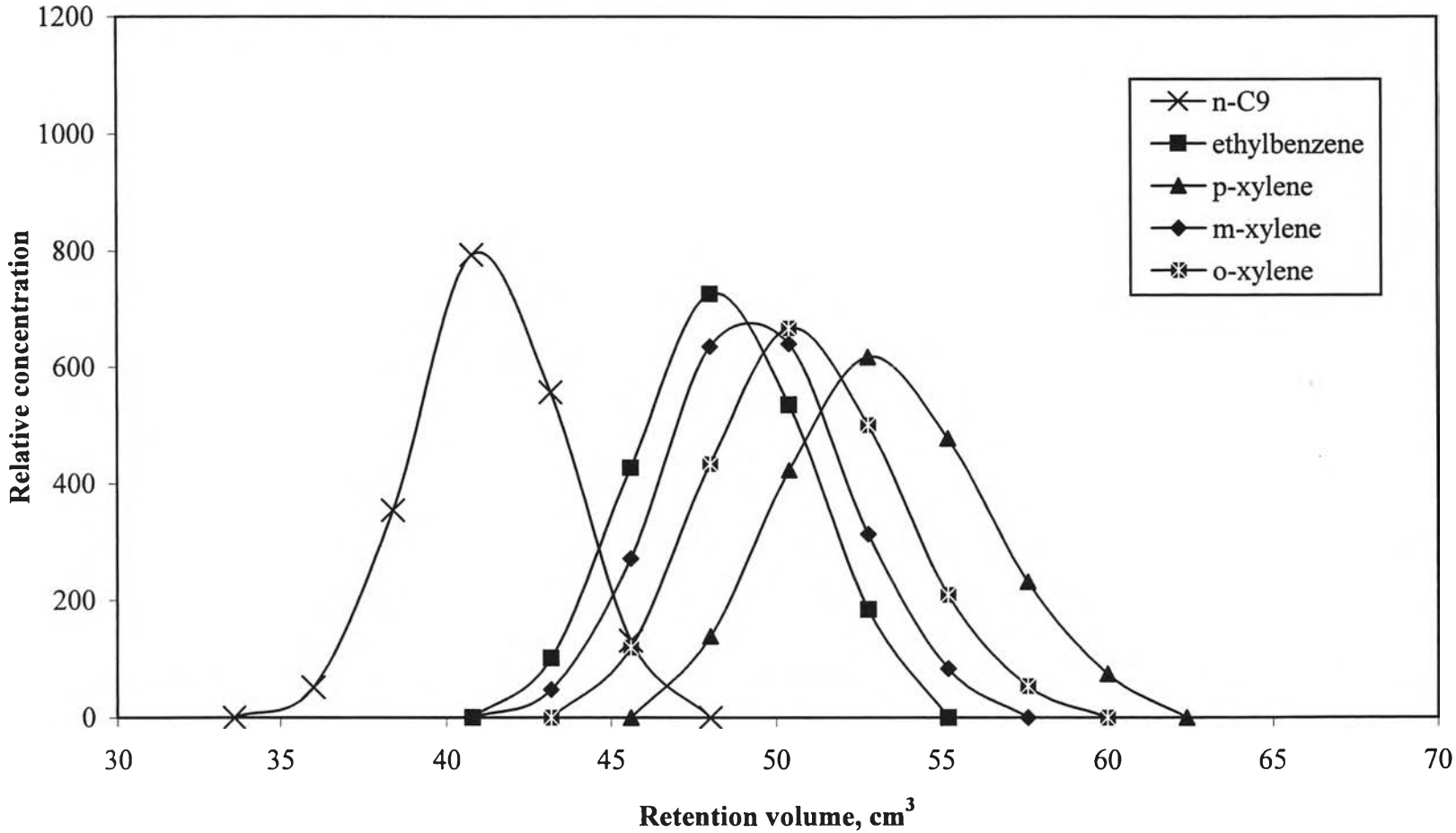

Figure 4.12 Dynamic adsorption: Multi-component pulse test on *BaY*.

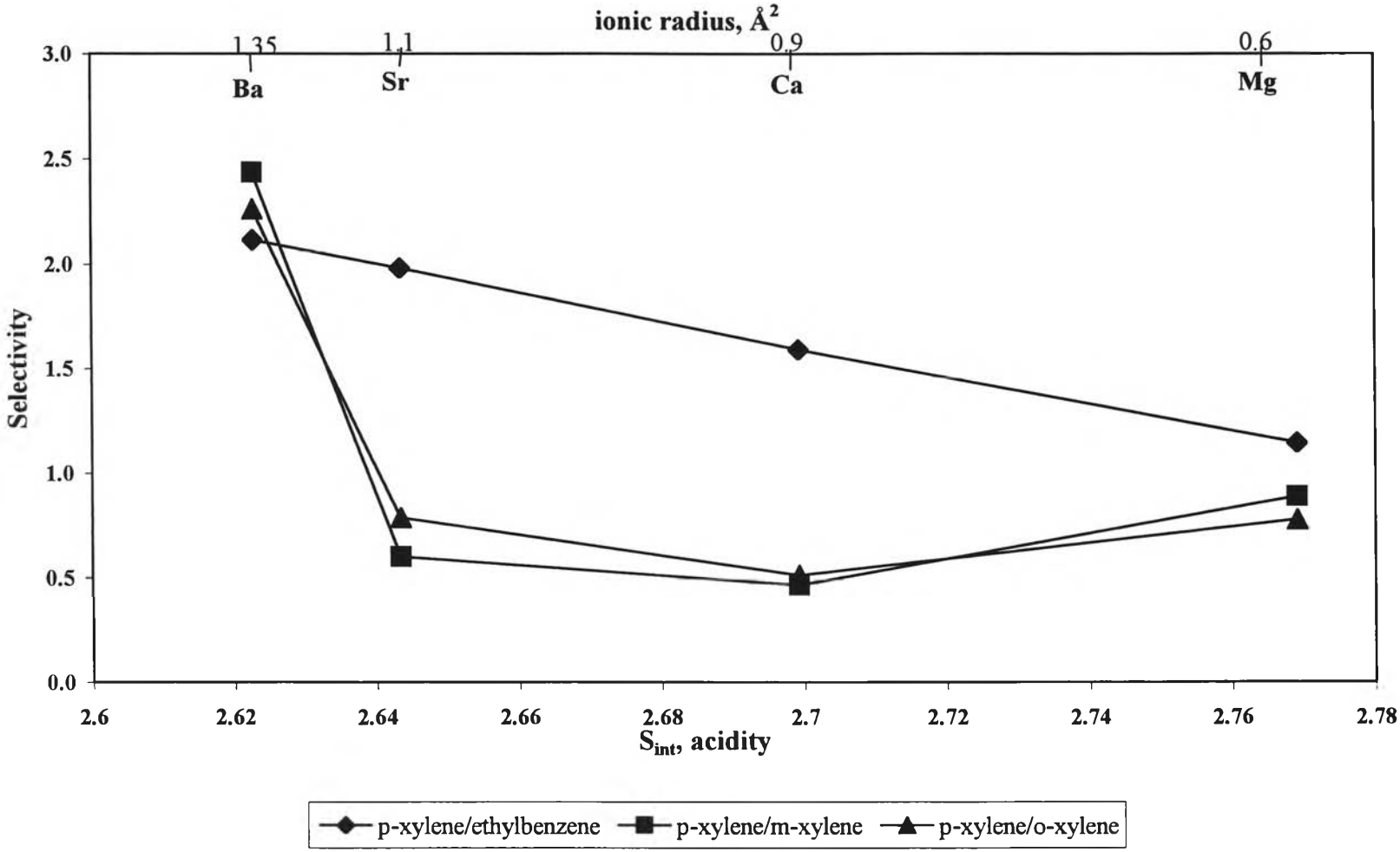

Figure 4.13 Relationship between *p* -xylene selectivity calculated from the Pulse Test experiments, cationic radius and 2.0X zeolite acidity.

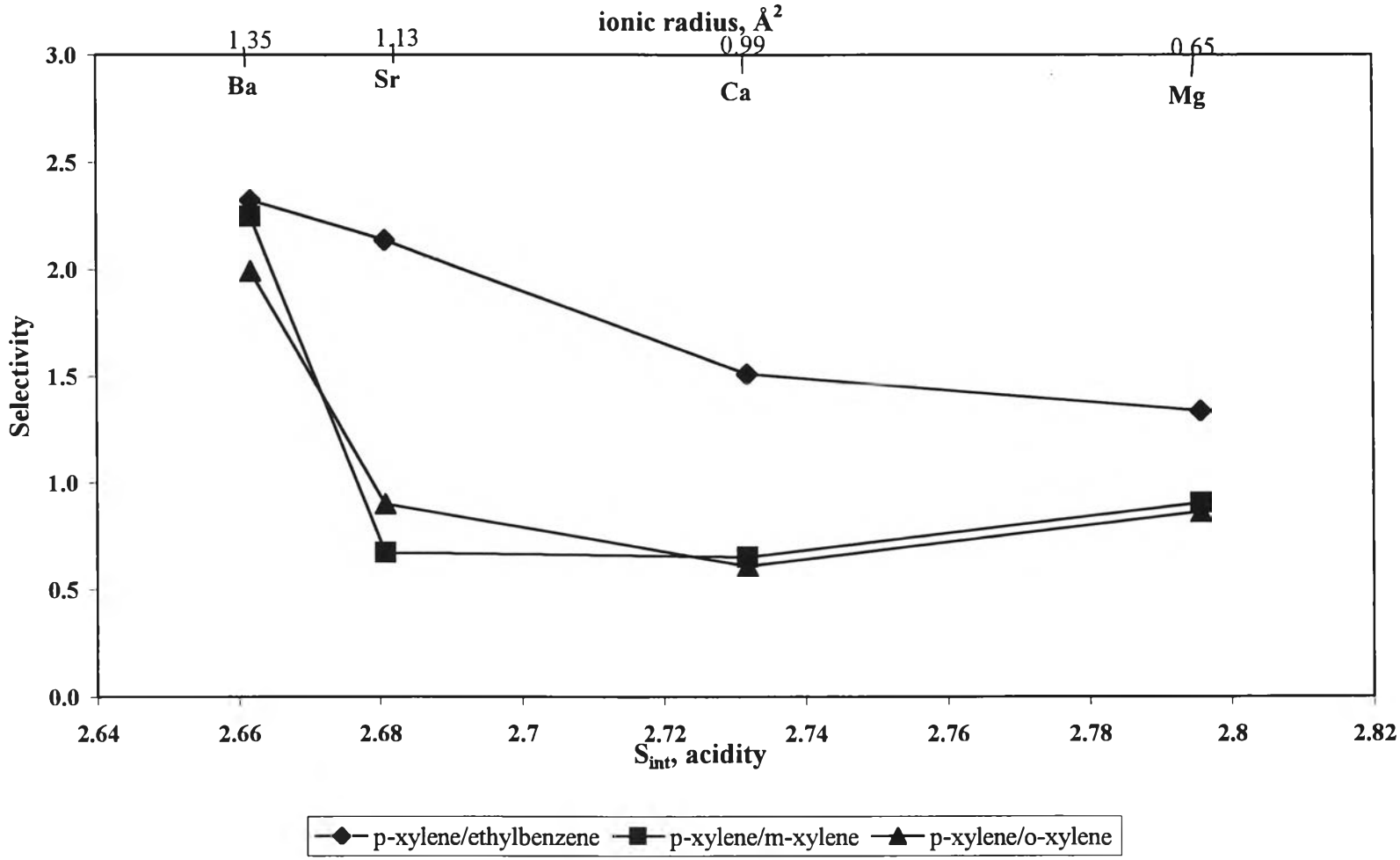

Figure 4.14 Relationship between *p* -xylene selectivity calculated from thePulse Test experiments, cationic radius and 2.5X zeolite acidity.

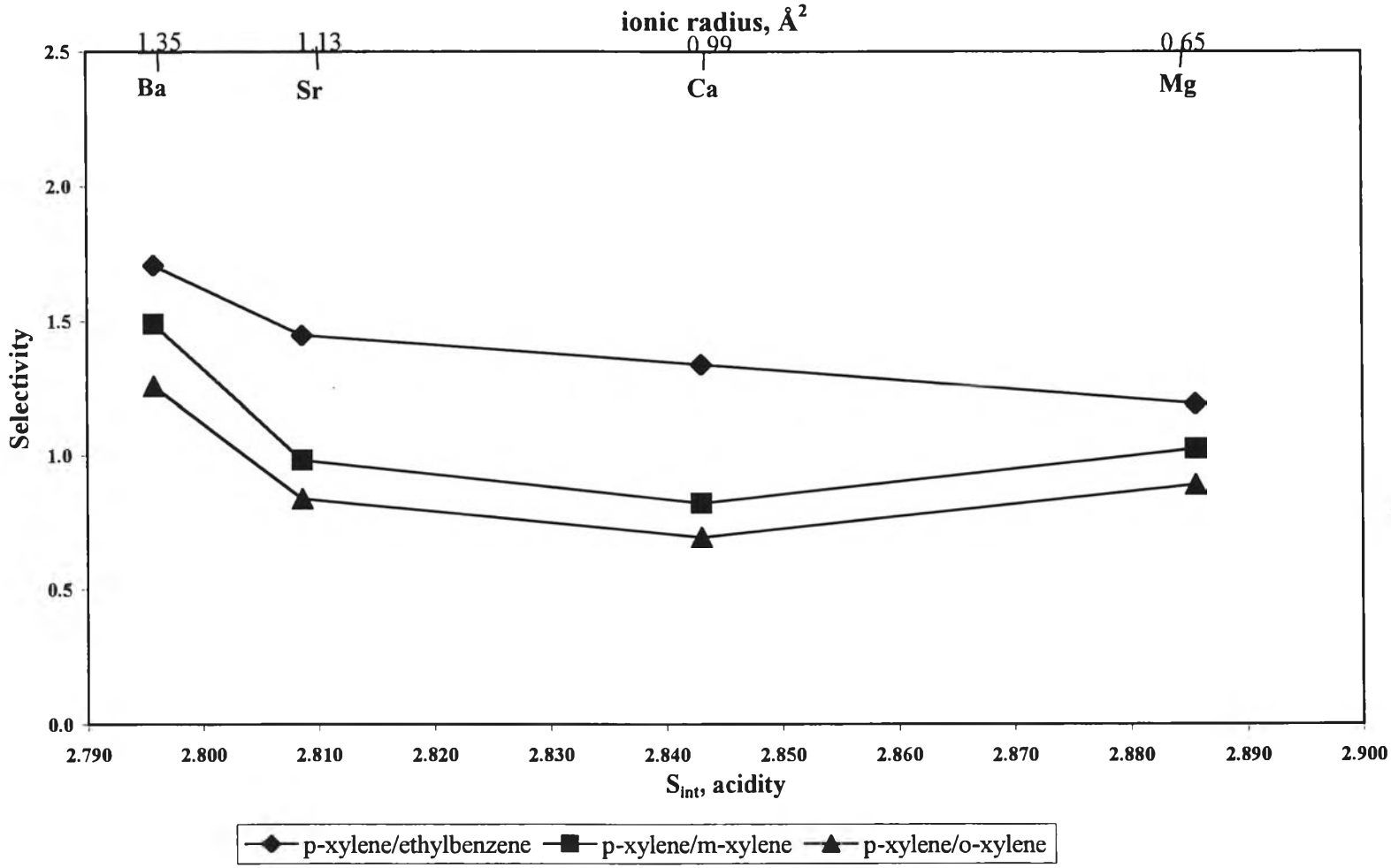

Figure 4.15 Relationship between *p* -xylene selectivity calculated from the Pulse Test experiments cationic radius and Y zeolite acidity.

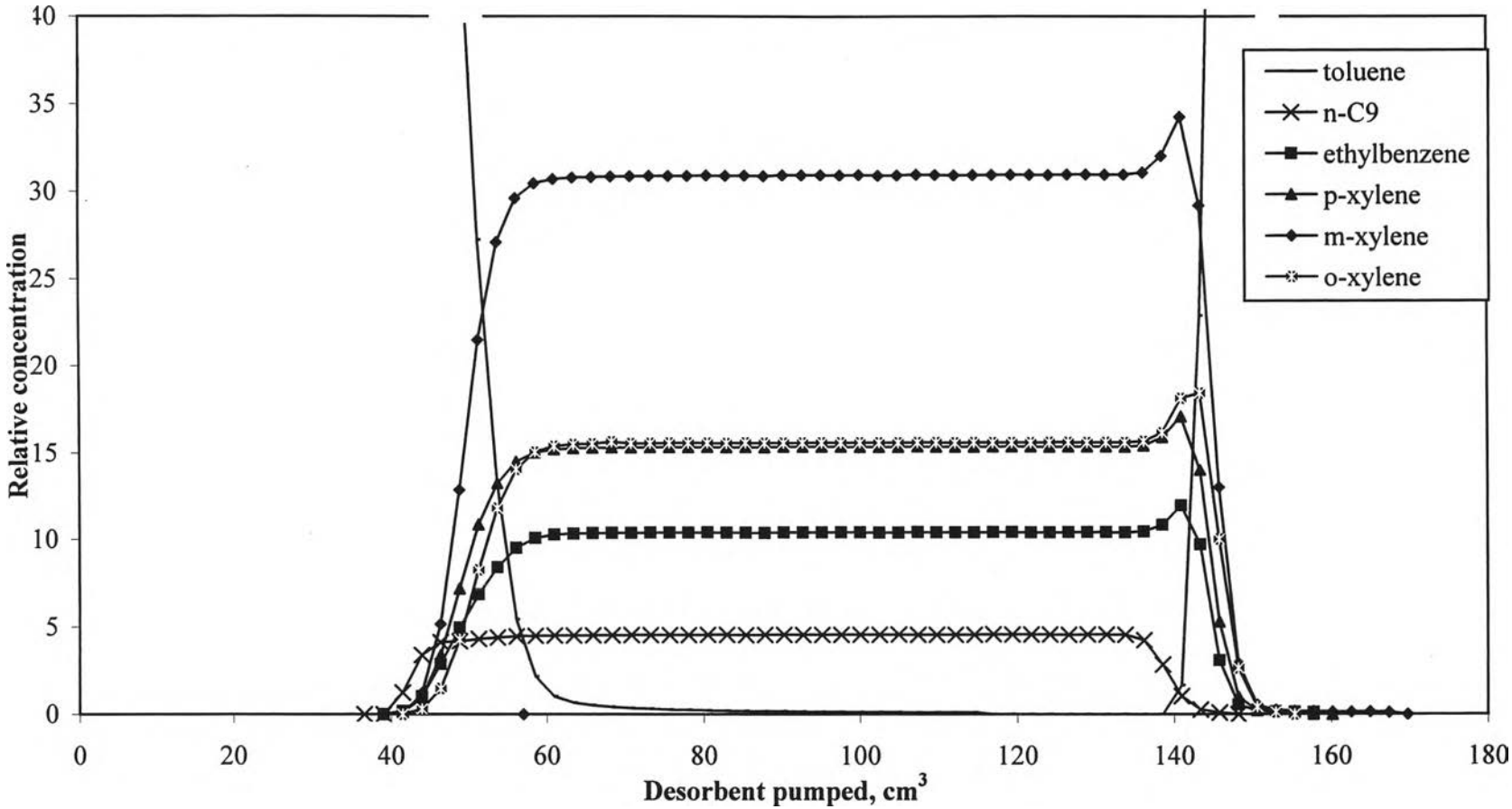

Figure 4.16 Dynamic adsorption: Breakthrough test on *Mg2.0X*.

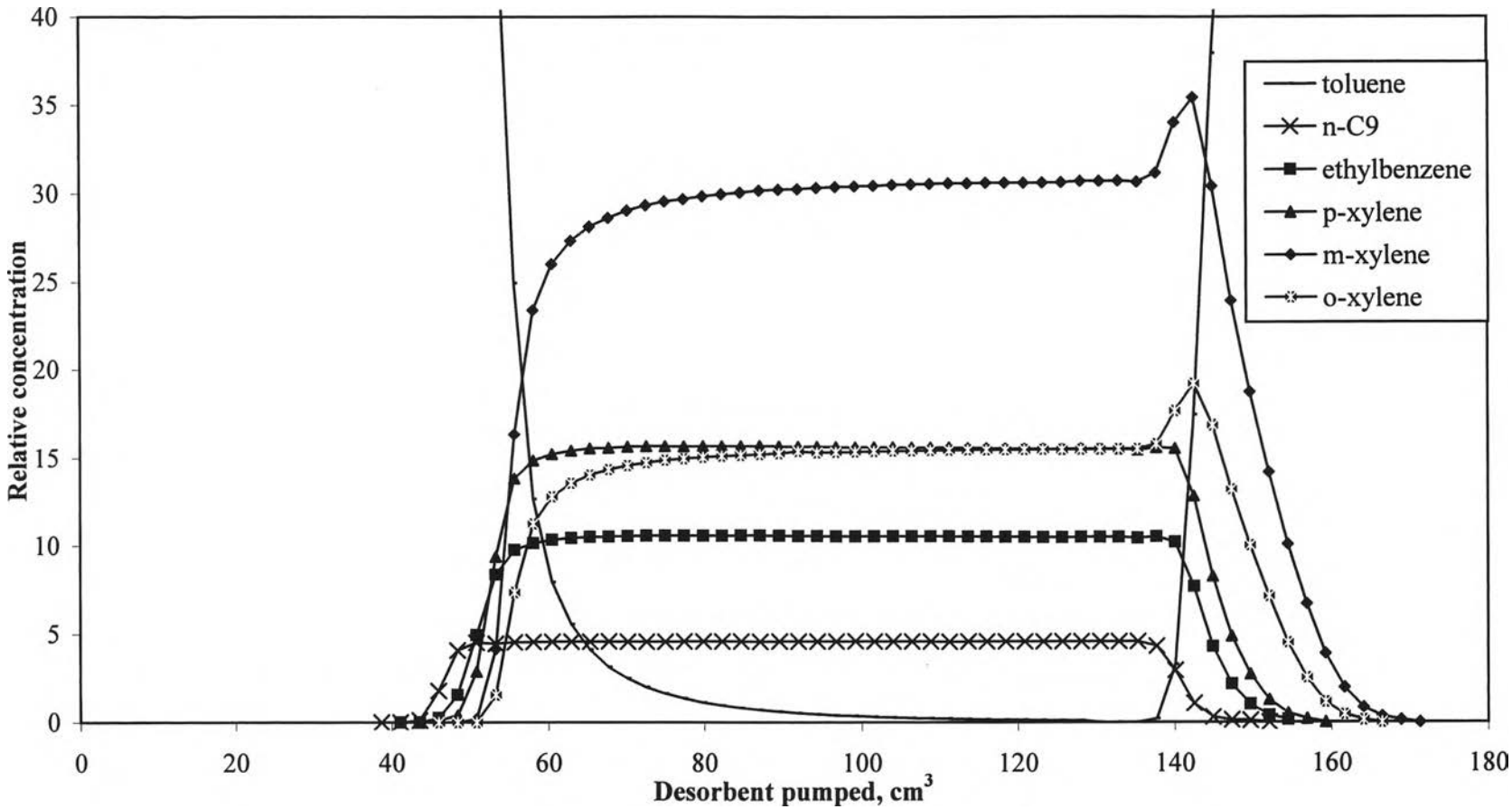

Figure 4.17 Dynamic adsorption: Breakthrough test on *Ca2.0X*.

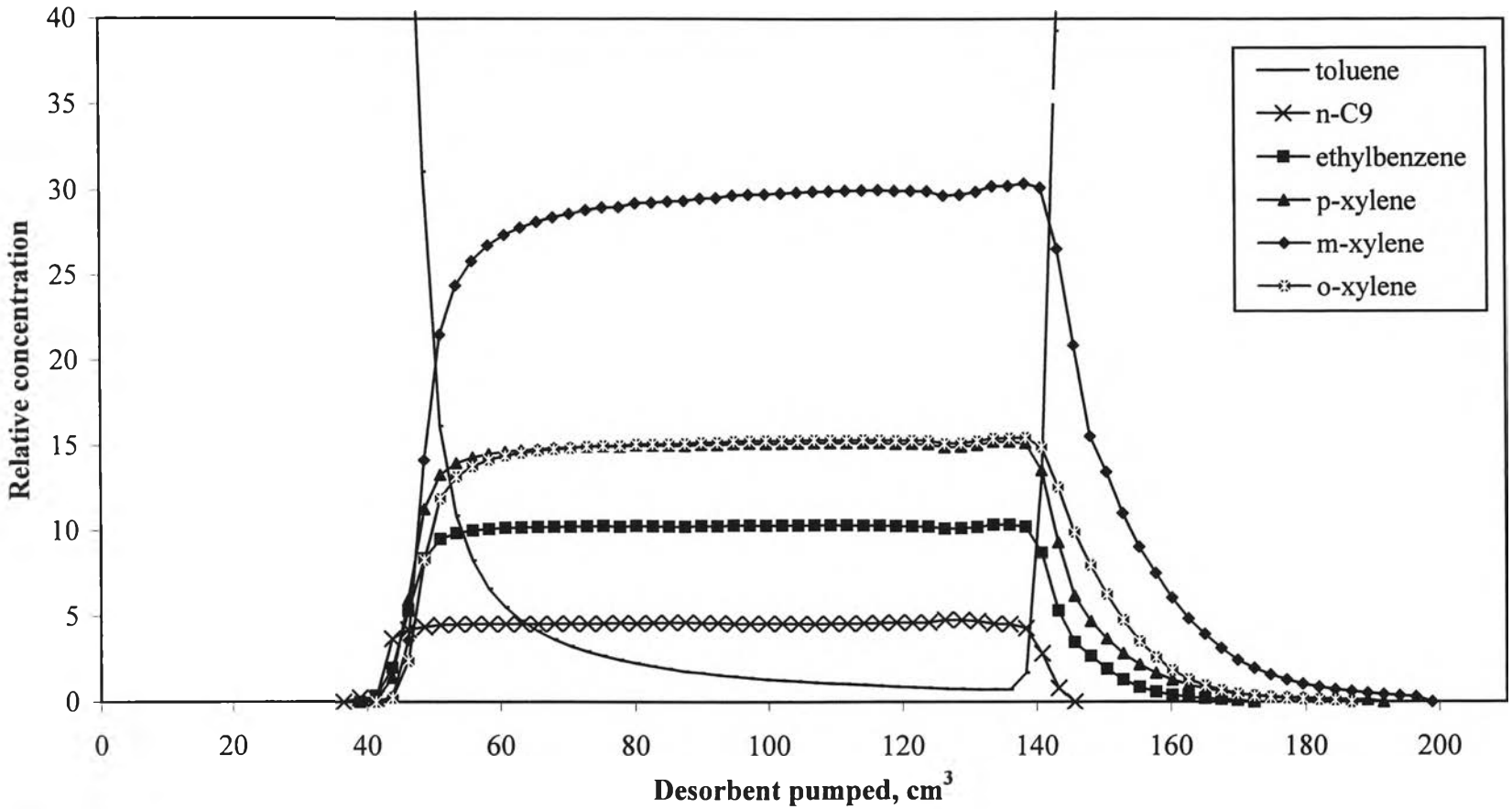

Figure 4.18 Dynamic adsorption: Breakthrough test on *Sr2.0X*.

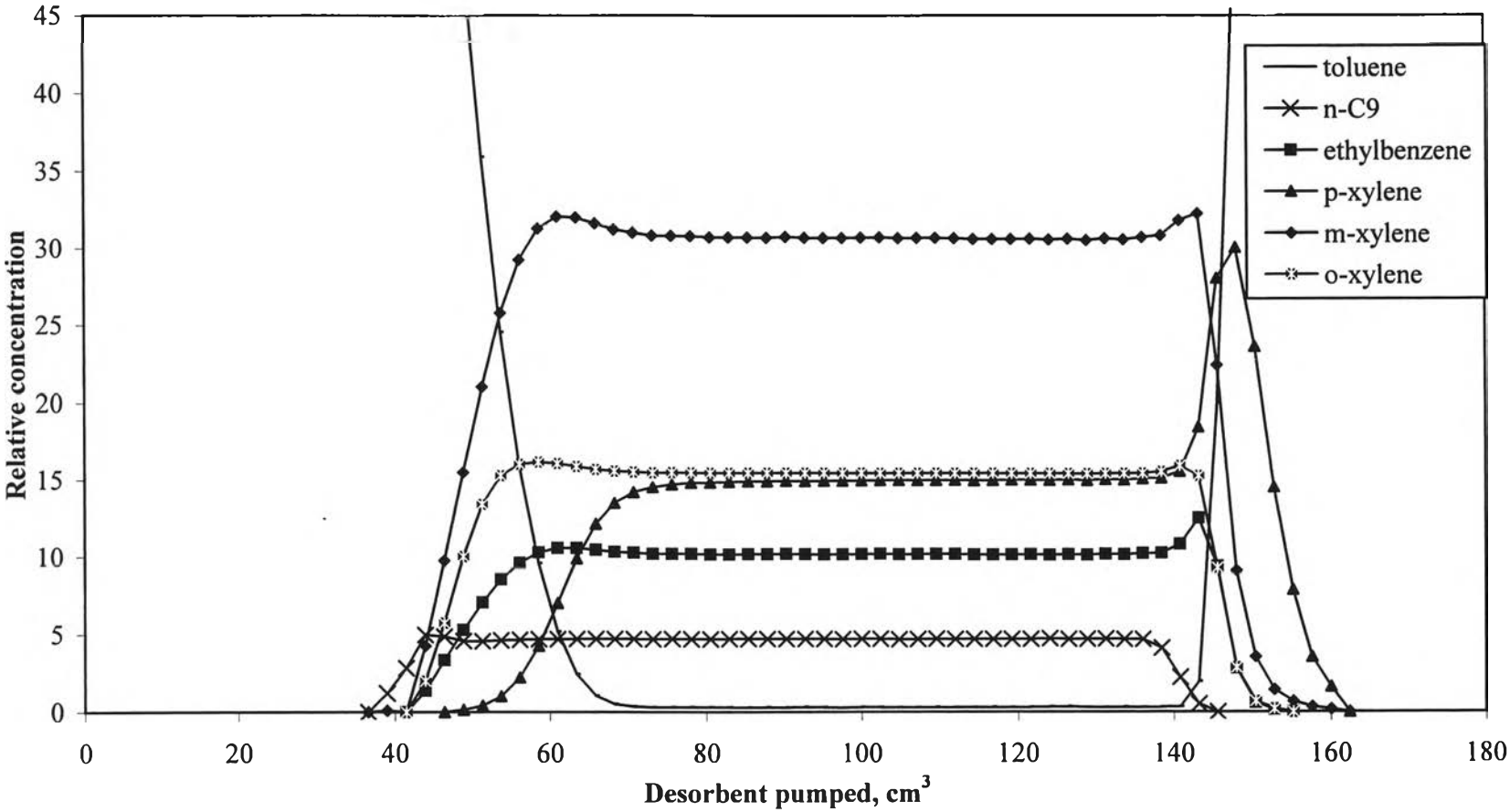

Figure 4.19 Dynamic adsorption: Breakthrough test on *Ba2.0X*.

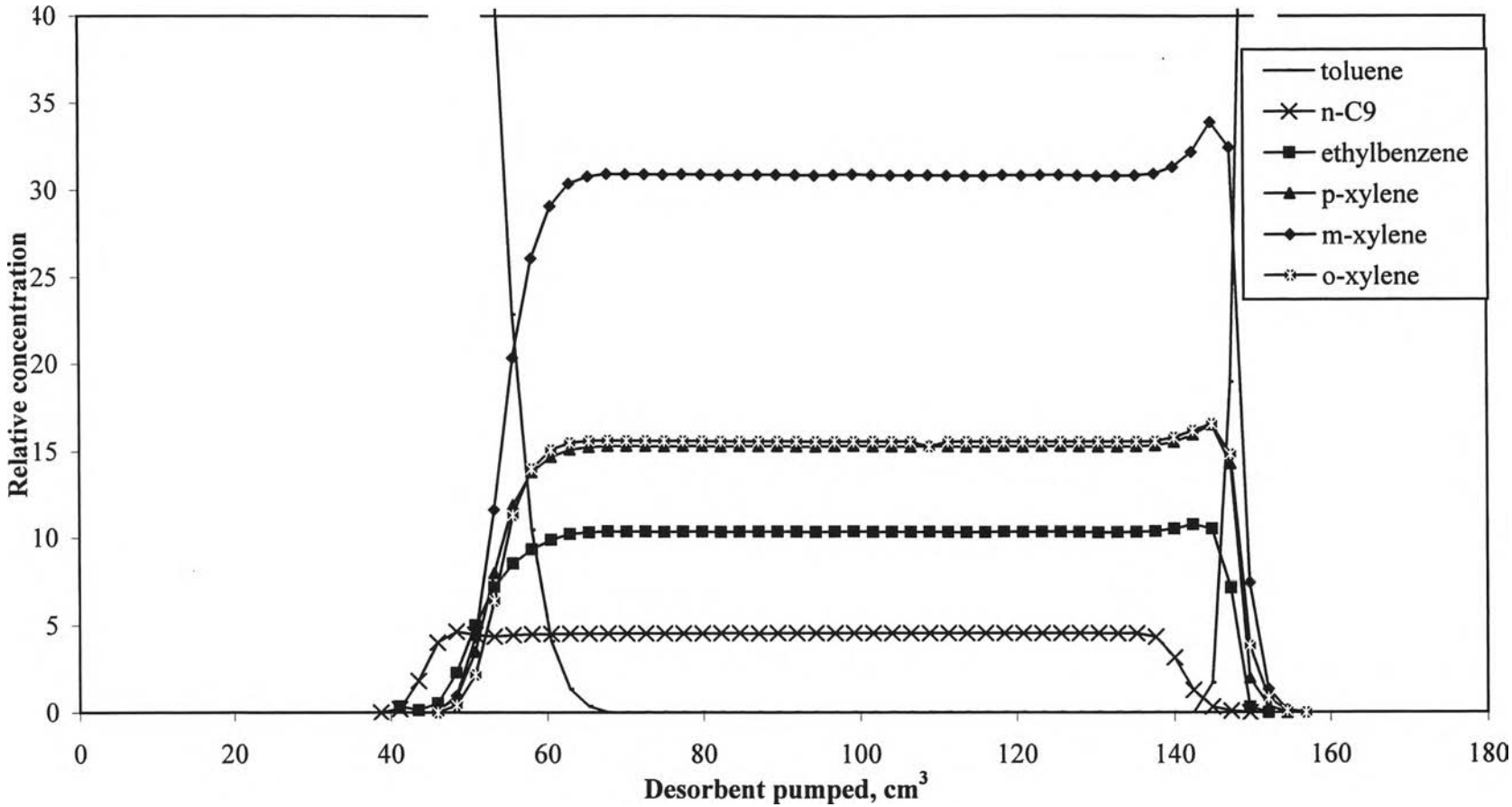

Figure 4.20 Dynamic adsorption: Breakthrough test on *Mg2.5X*.

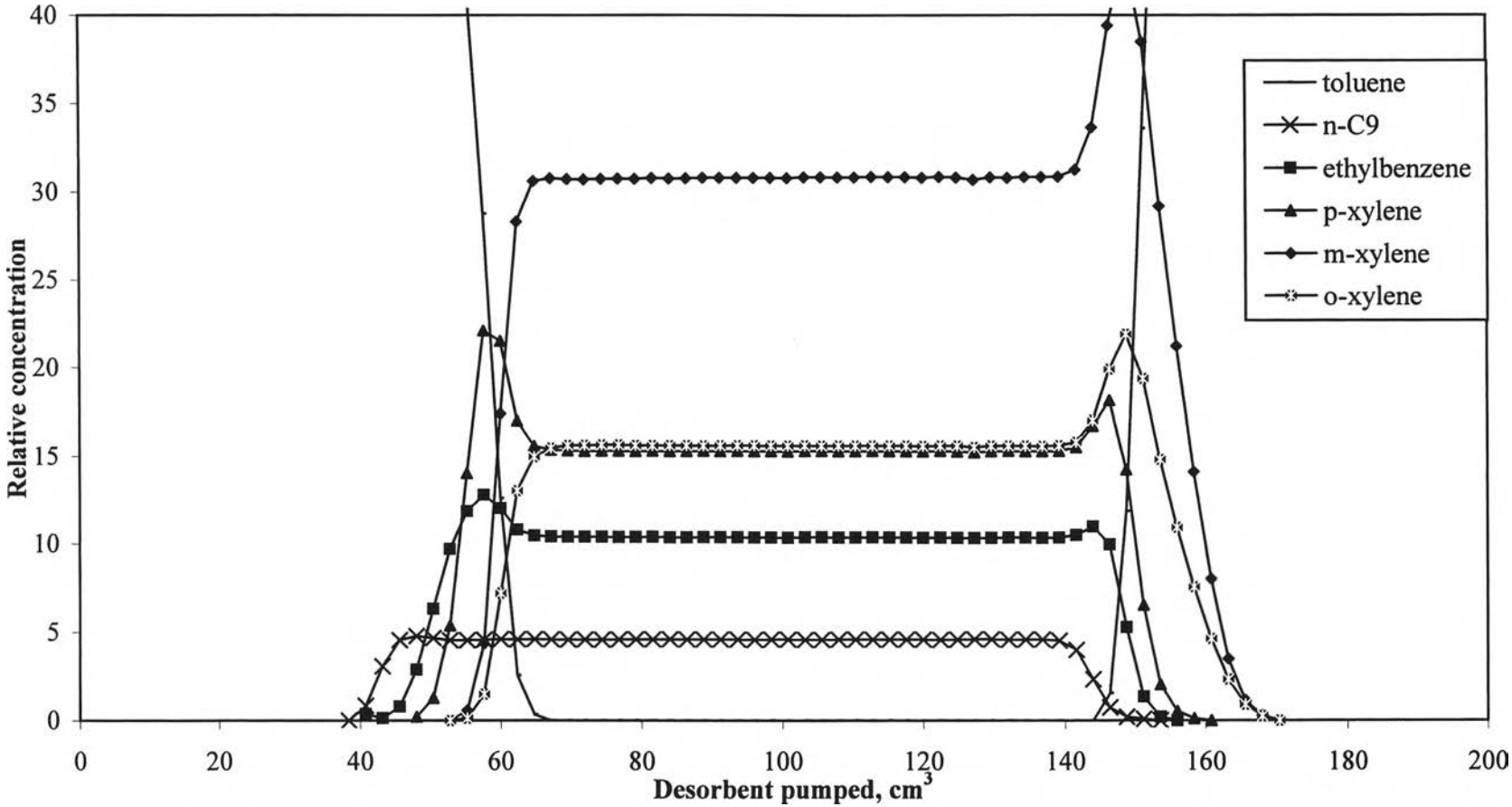

Figure 4.21 Dynamic adsorption: Breakthrough test on *Ca2.5X*.

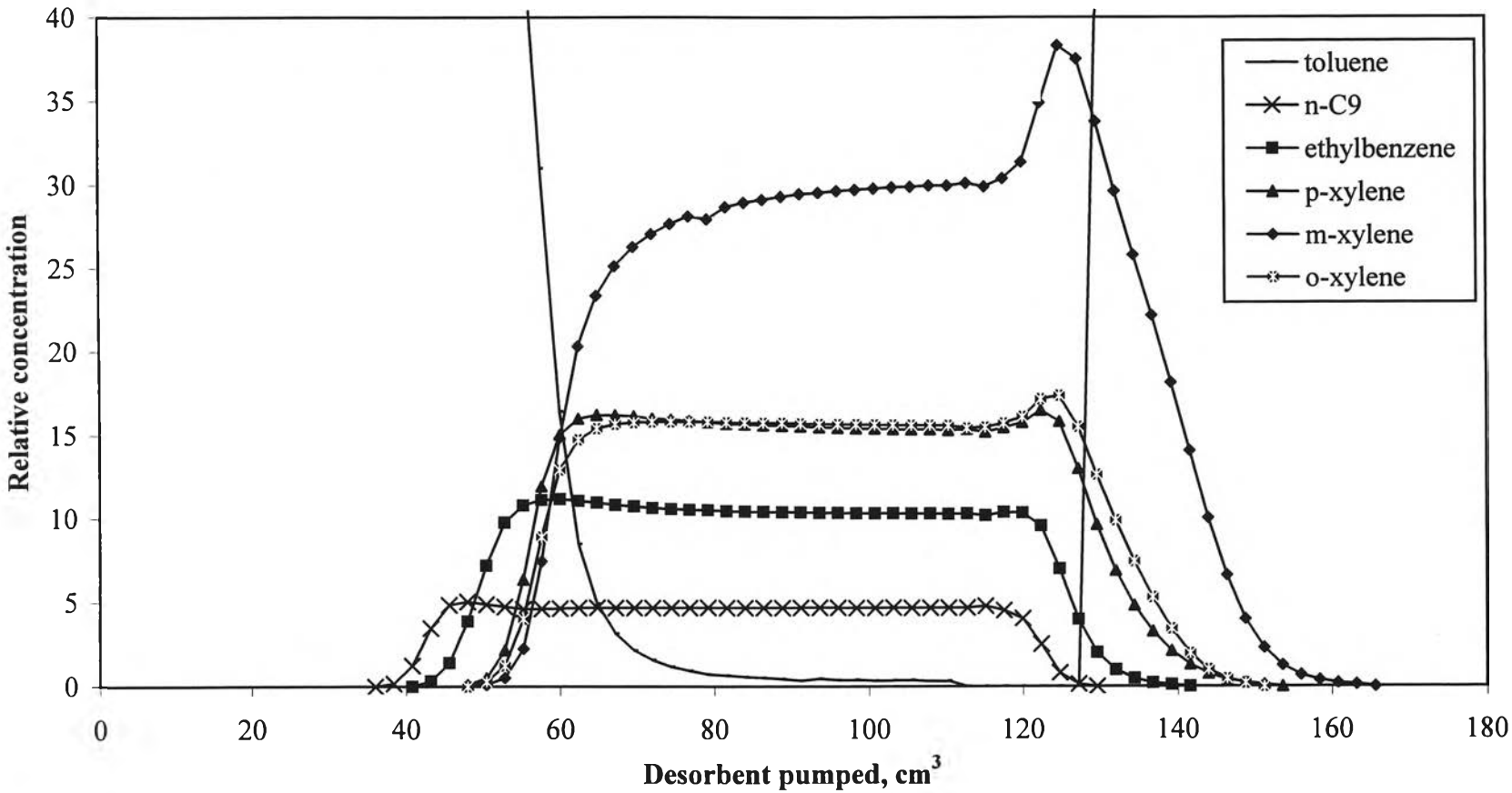

Figure 4.22 Dynamic adsorption: Breakthrough test on *Sr2.5X*.

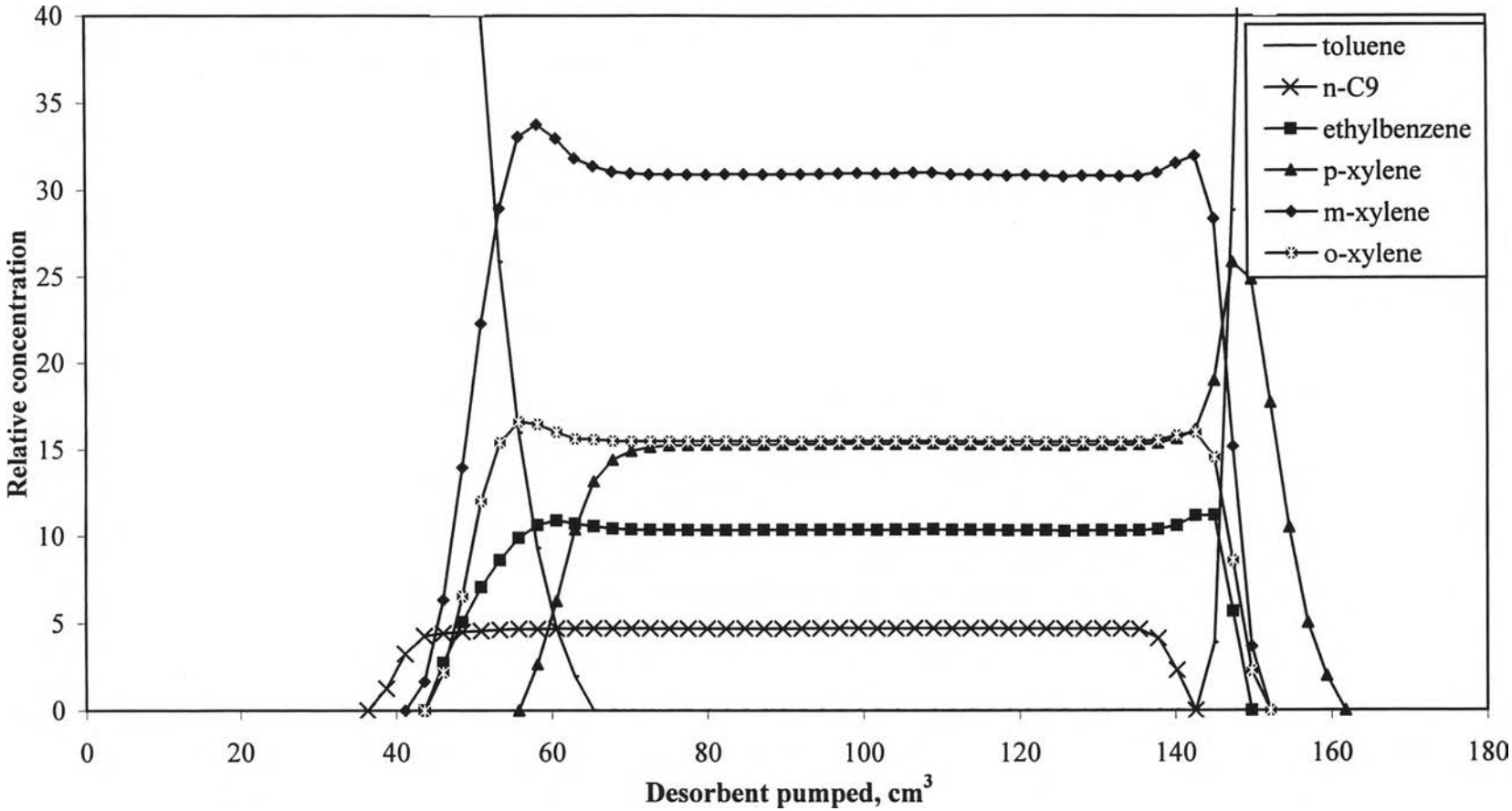

Figure 4.23 Dynamic adsorption: Breakthrough test on *Ba2.5X*.

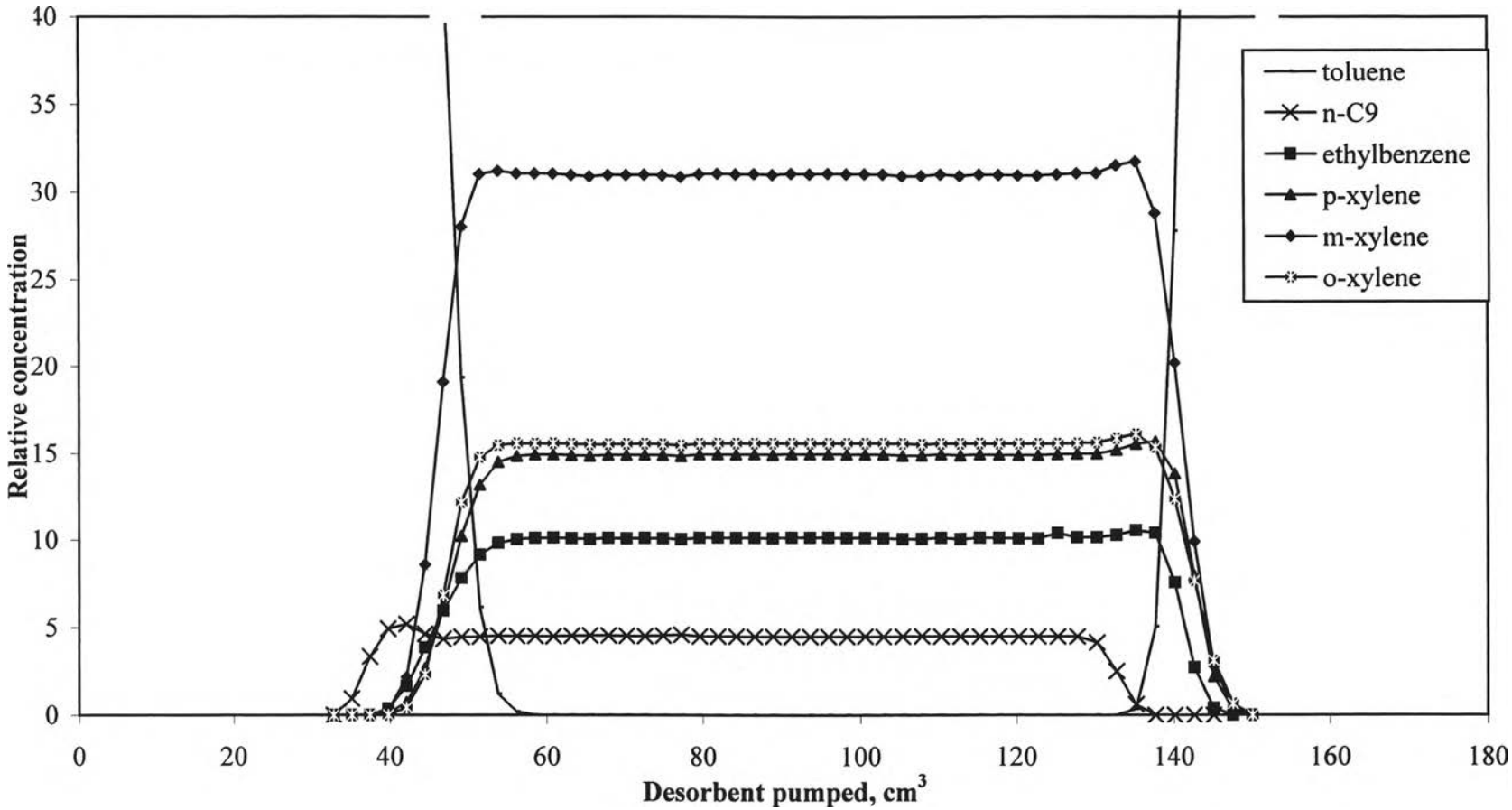

Figure 4.24 Dynamic adsorption: Breakthrough test on *MgY*.

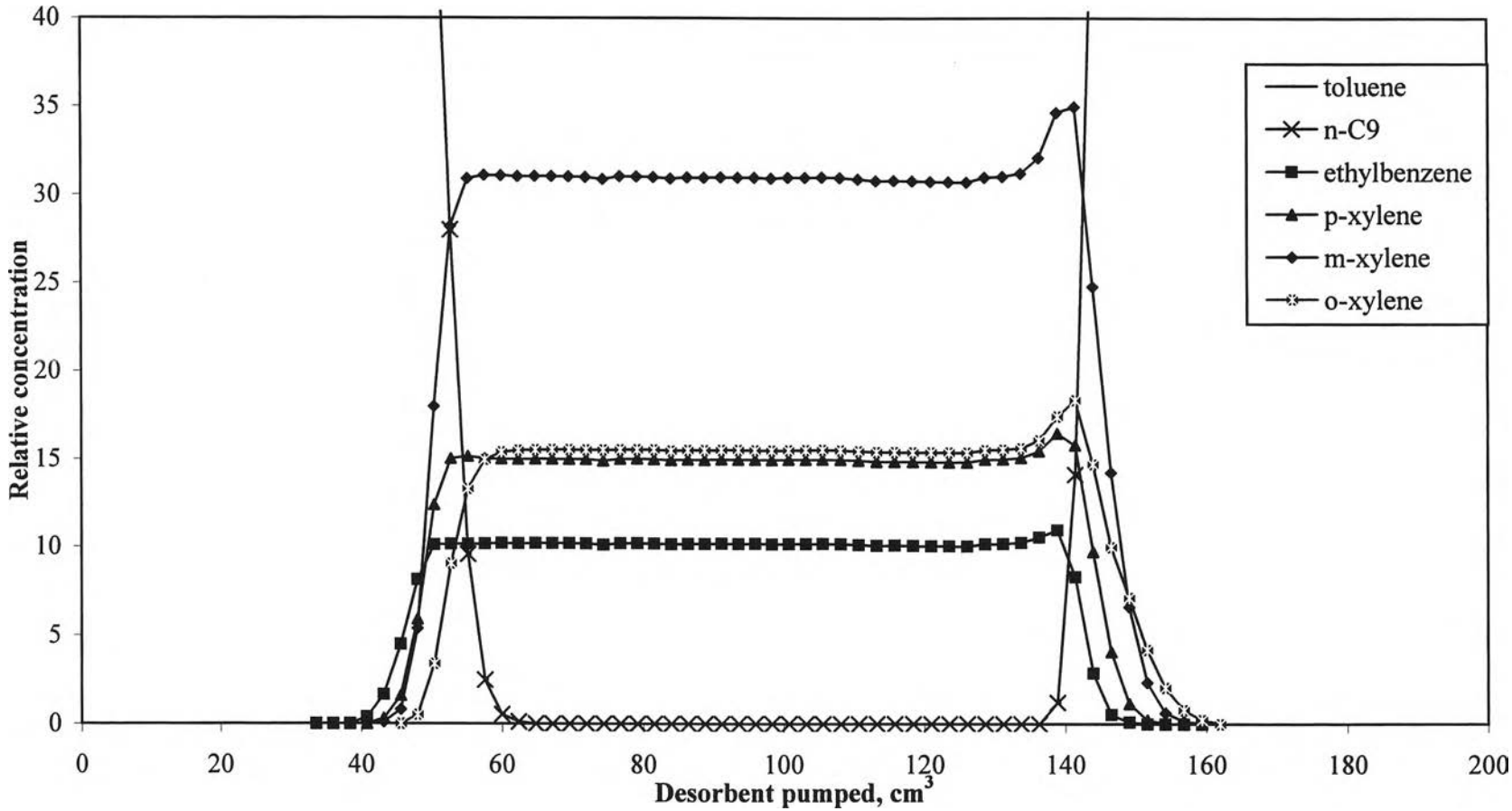

Figure 4.25 Dynamic adsorption: Breakthrough test on *CaY*.

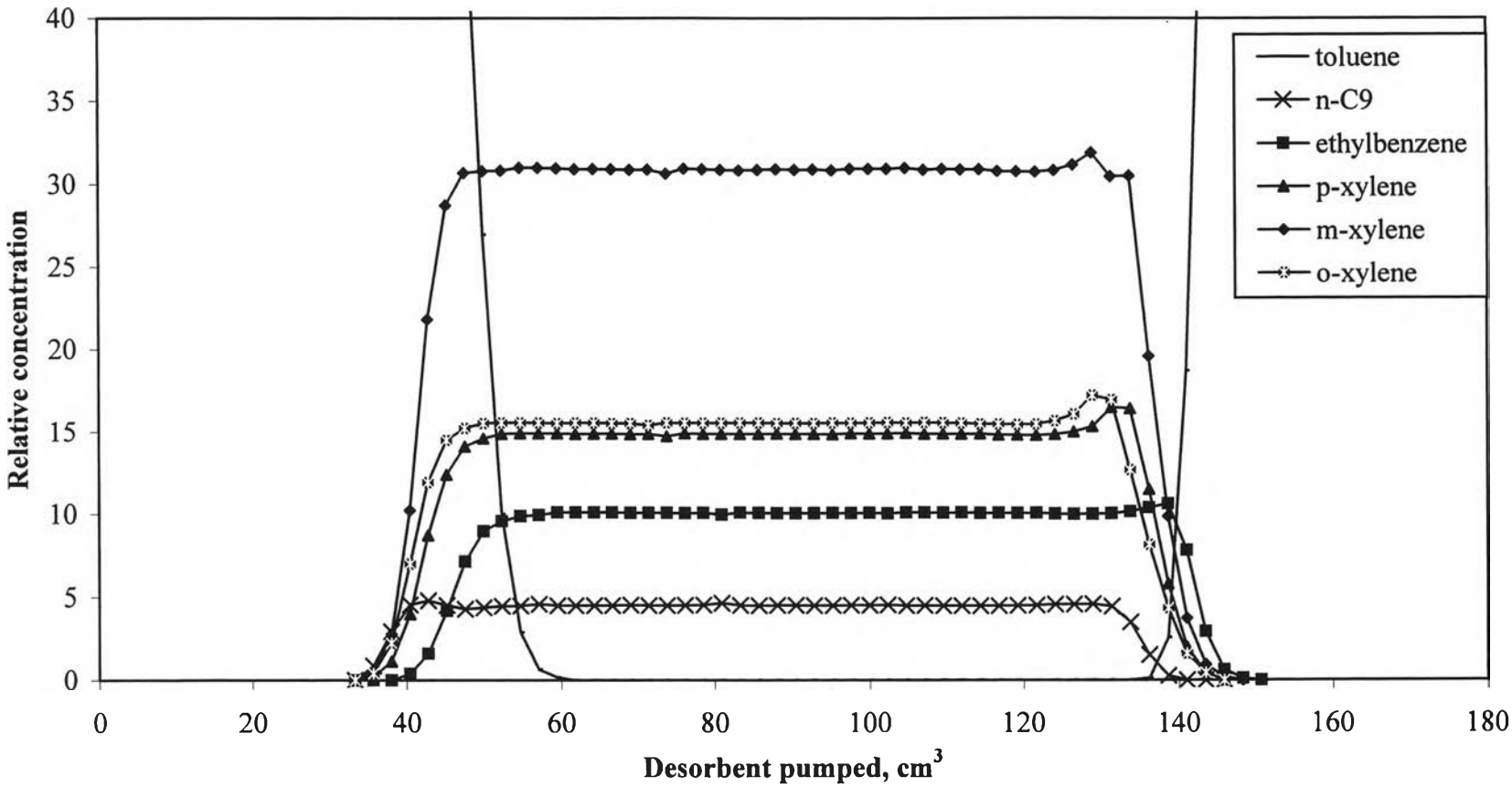

Figure 4.26 Dynamic adsorption: Breakthrough test on *SrY*.

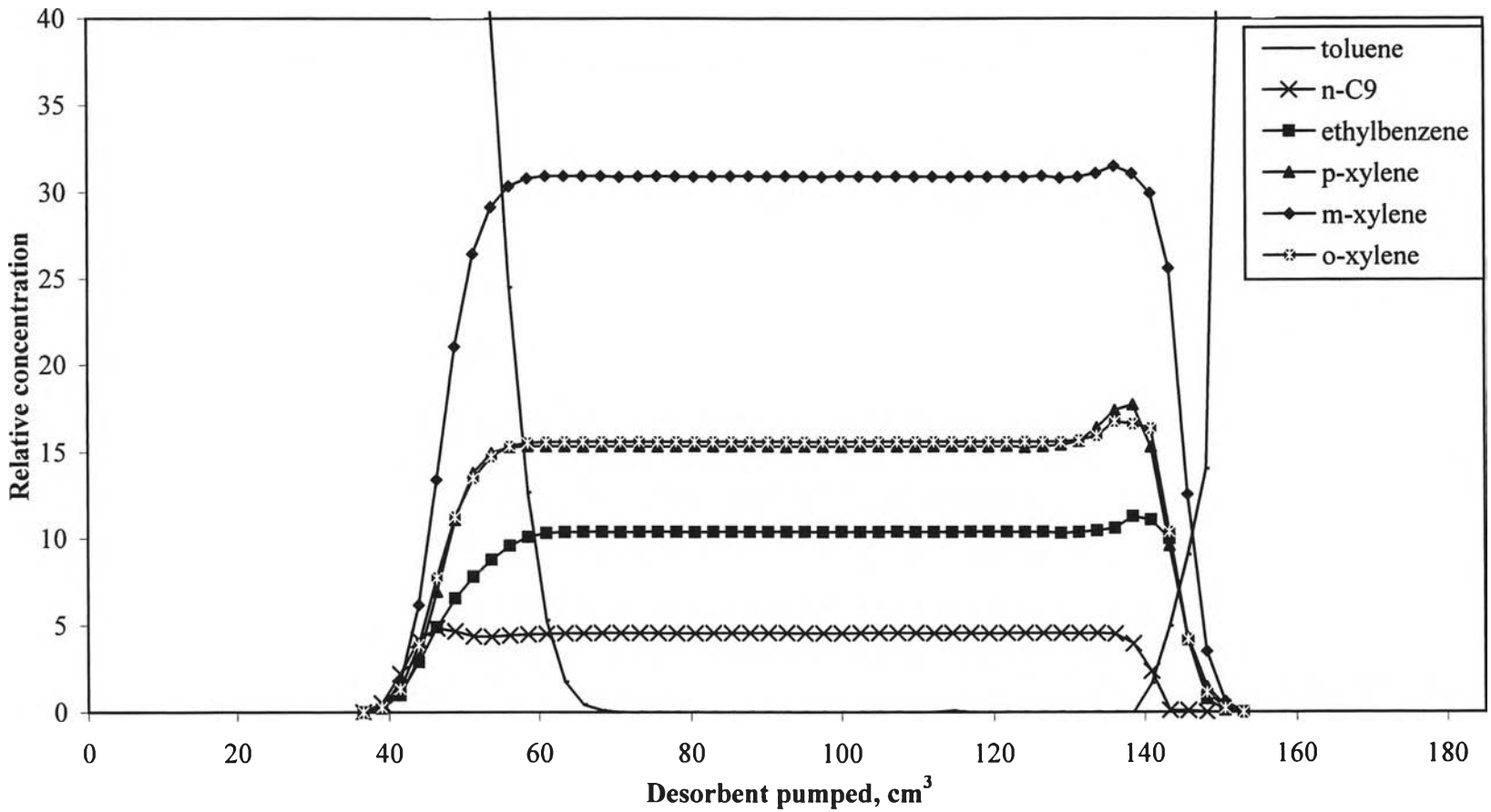

Figure 4.27 Dynamic adsorption: Breakthrough test on *BaY*.

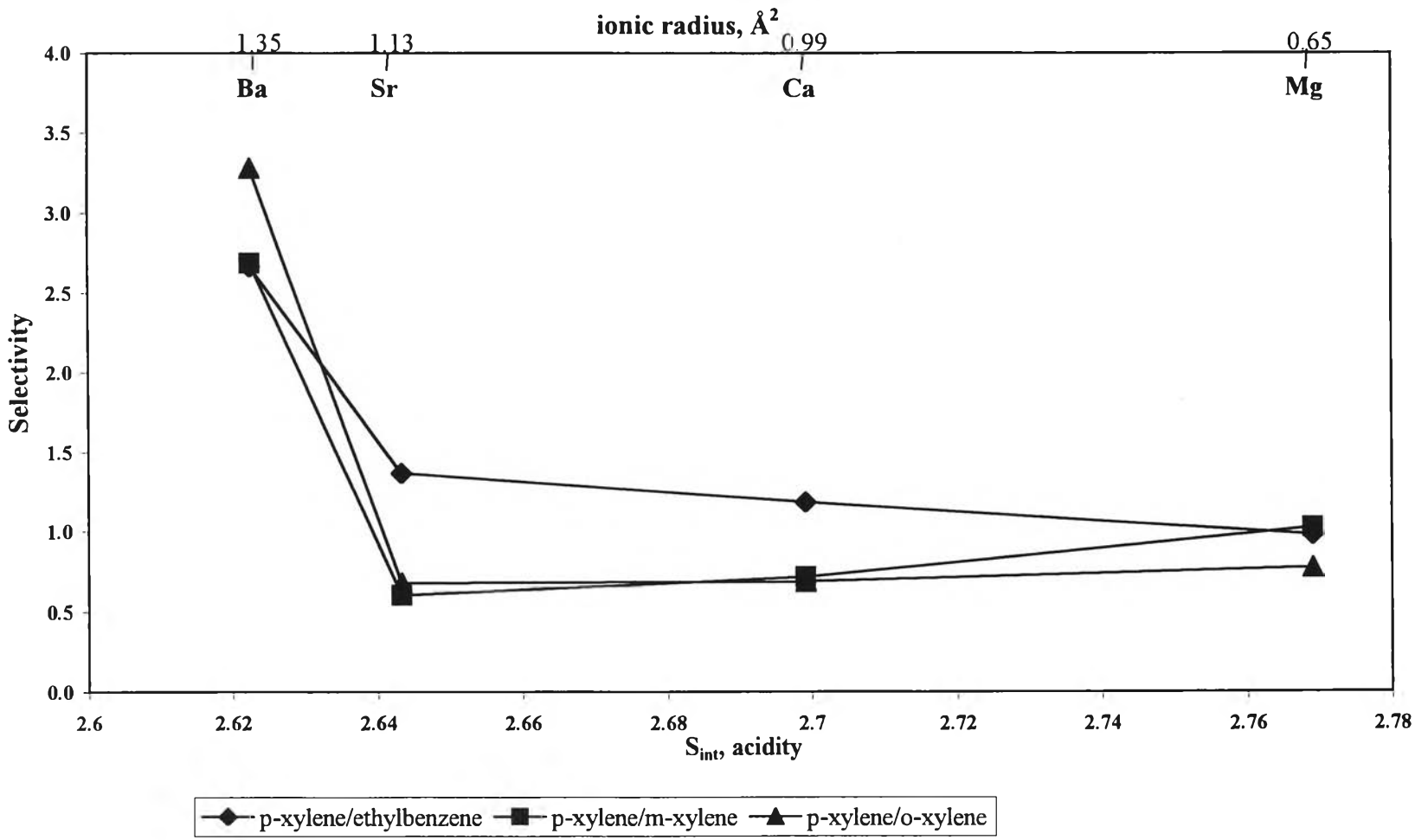

Figure 4.28 Relationship between *p* -xylene selectivity calculated from the Breakthrough experiments cationic radius and 2.0X zeolite acidity.

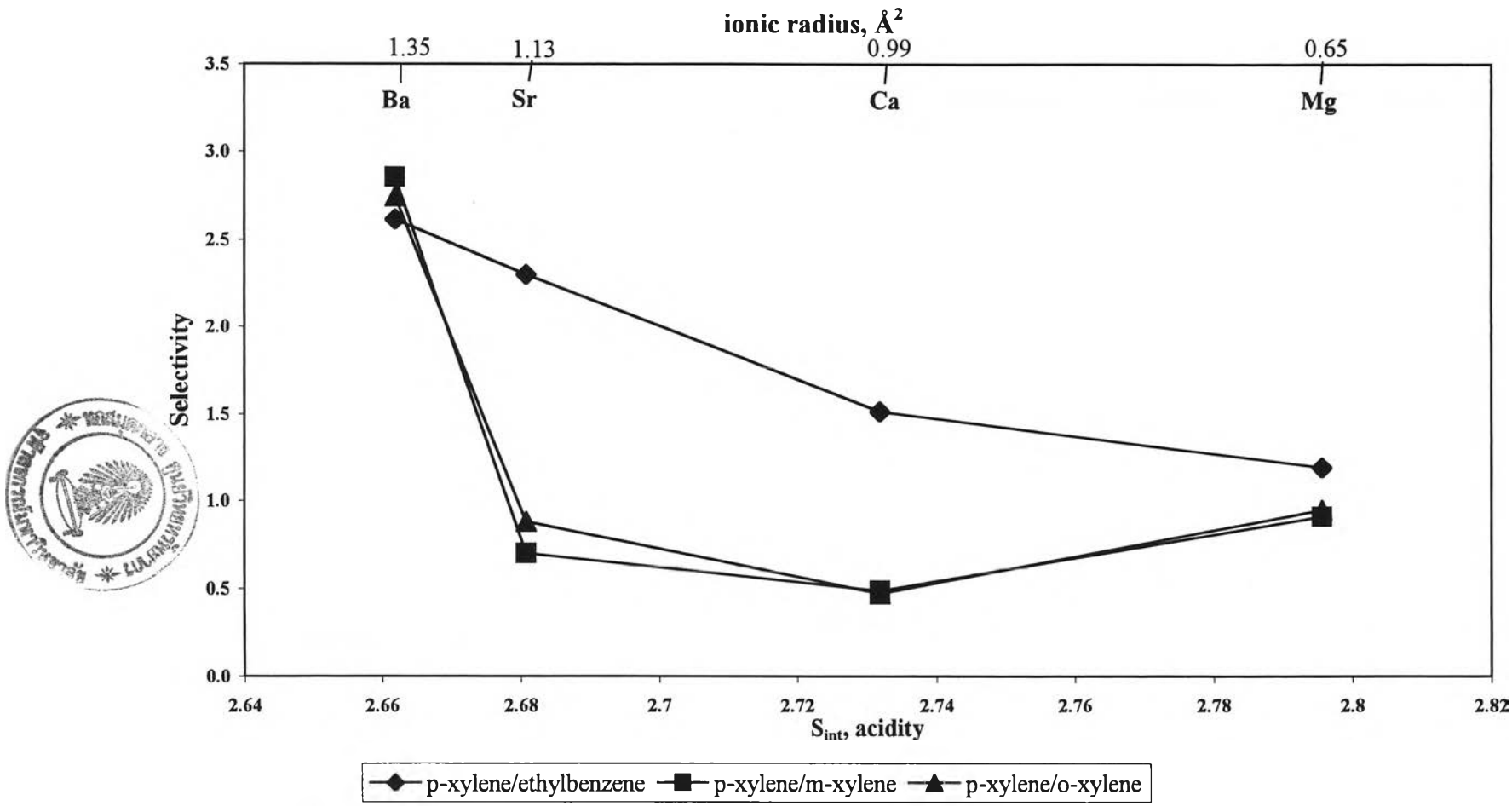

Figure 4.29 Relationship between *p* -xylene selectivity calculated from the Breakthrough experiments cationic radius and 2.5X zeolite acidity.

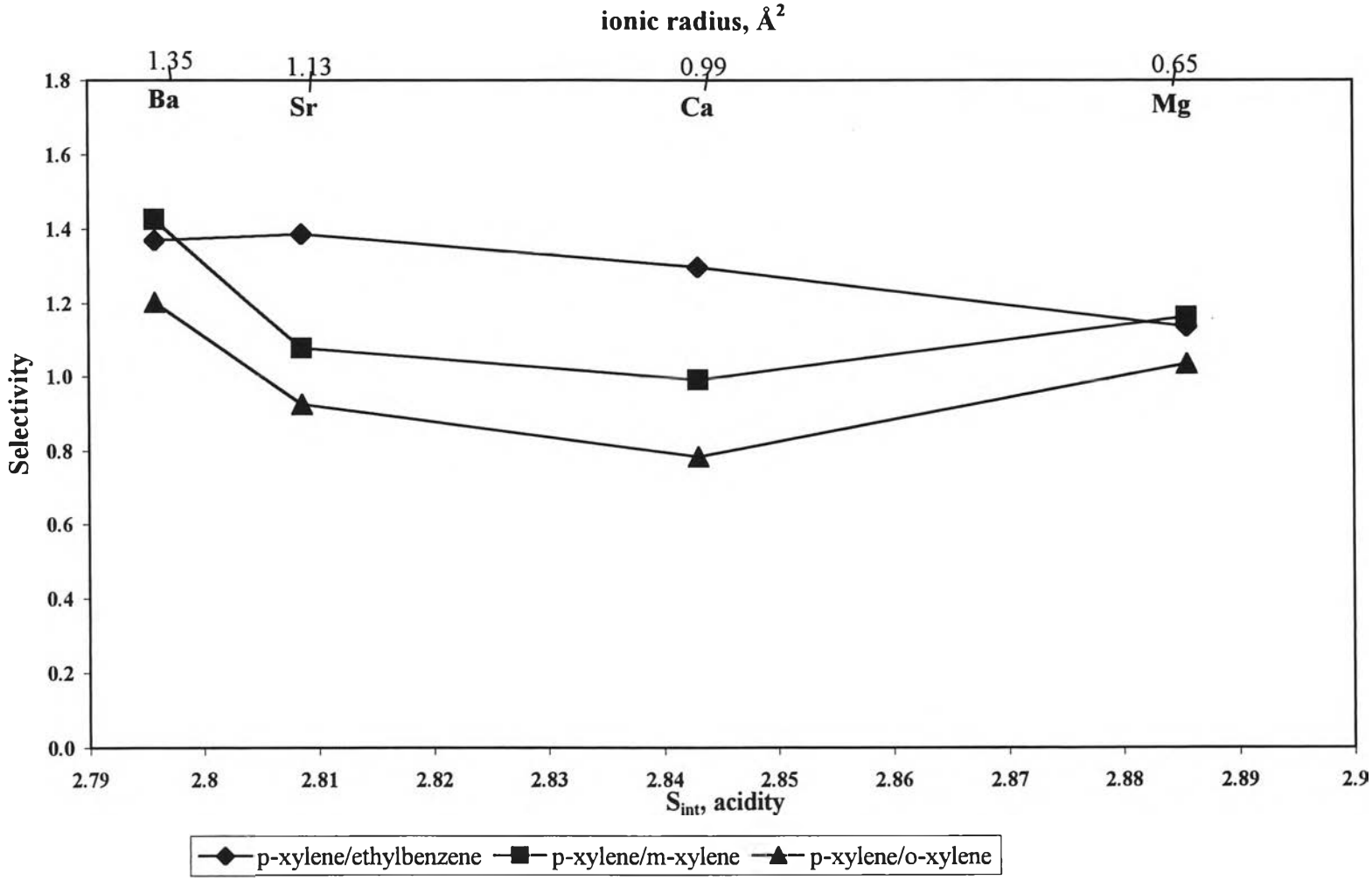

Figure 4.30 Realtionship between *p* -xylene selectivity calculated from the Breakthrough experiments cationic radius and Y zeolite acidity.

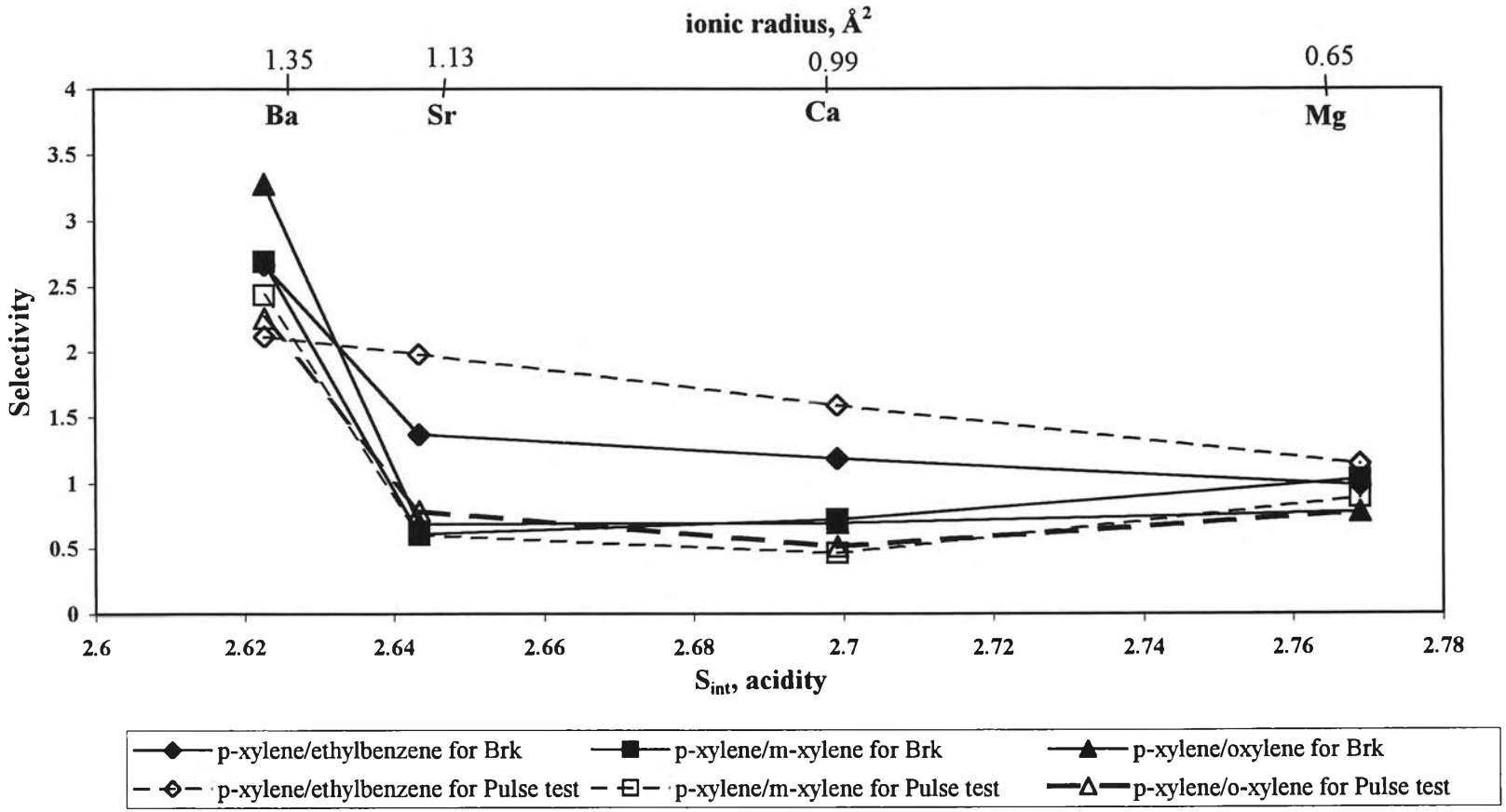

Figure 4.31 Comparison of p-xylene selectivity calculated from the Breakthrough and Pulse Test experiments for 2.0X zeolite.

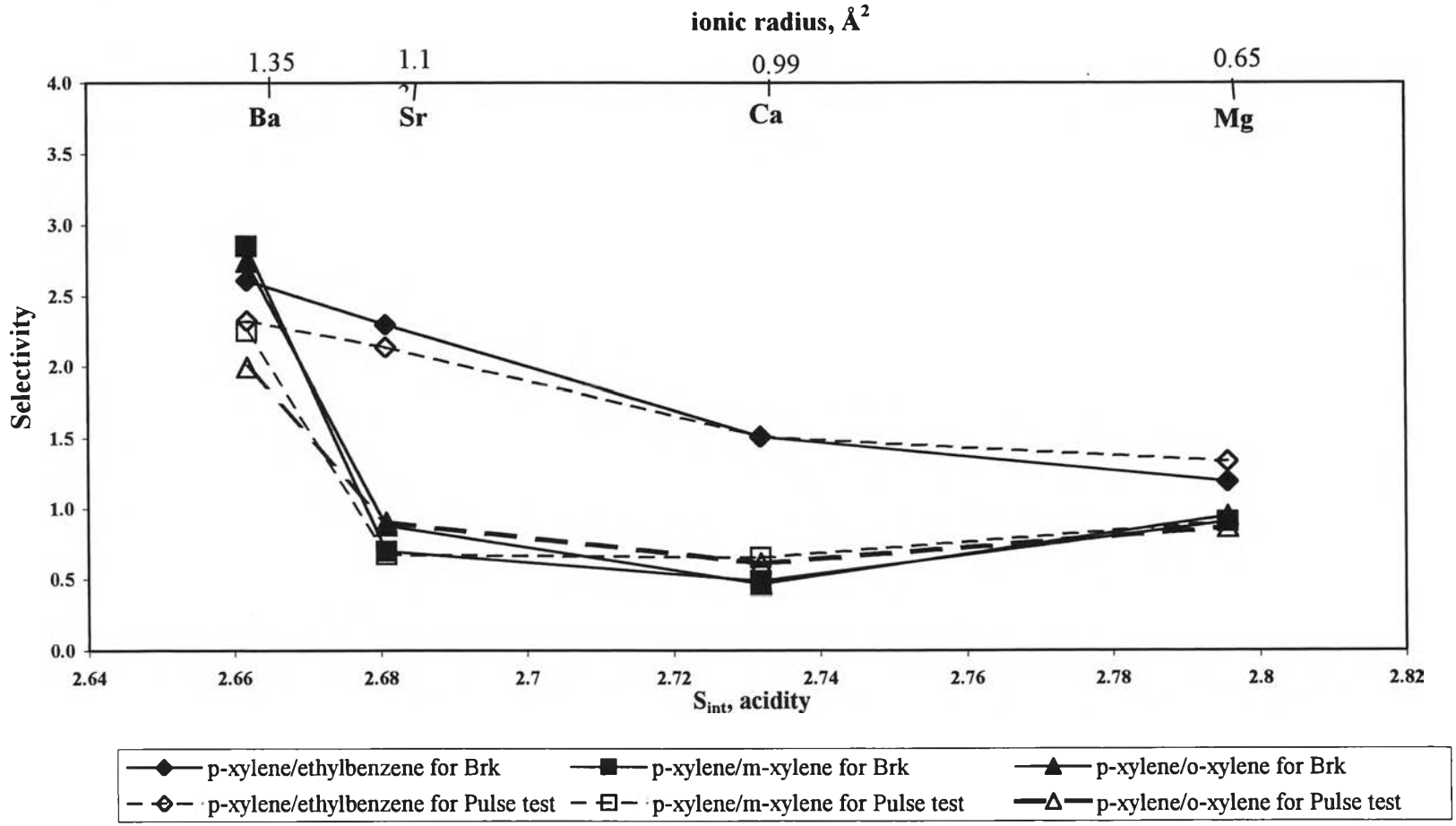

Figure 4.32 Comparison of p-xylene selectivity calculated from the Breakthrough and Pulse Test experiments for 2.5X Zeolite.

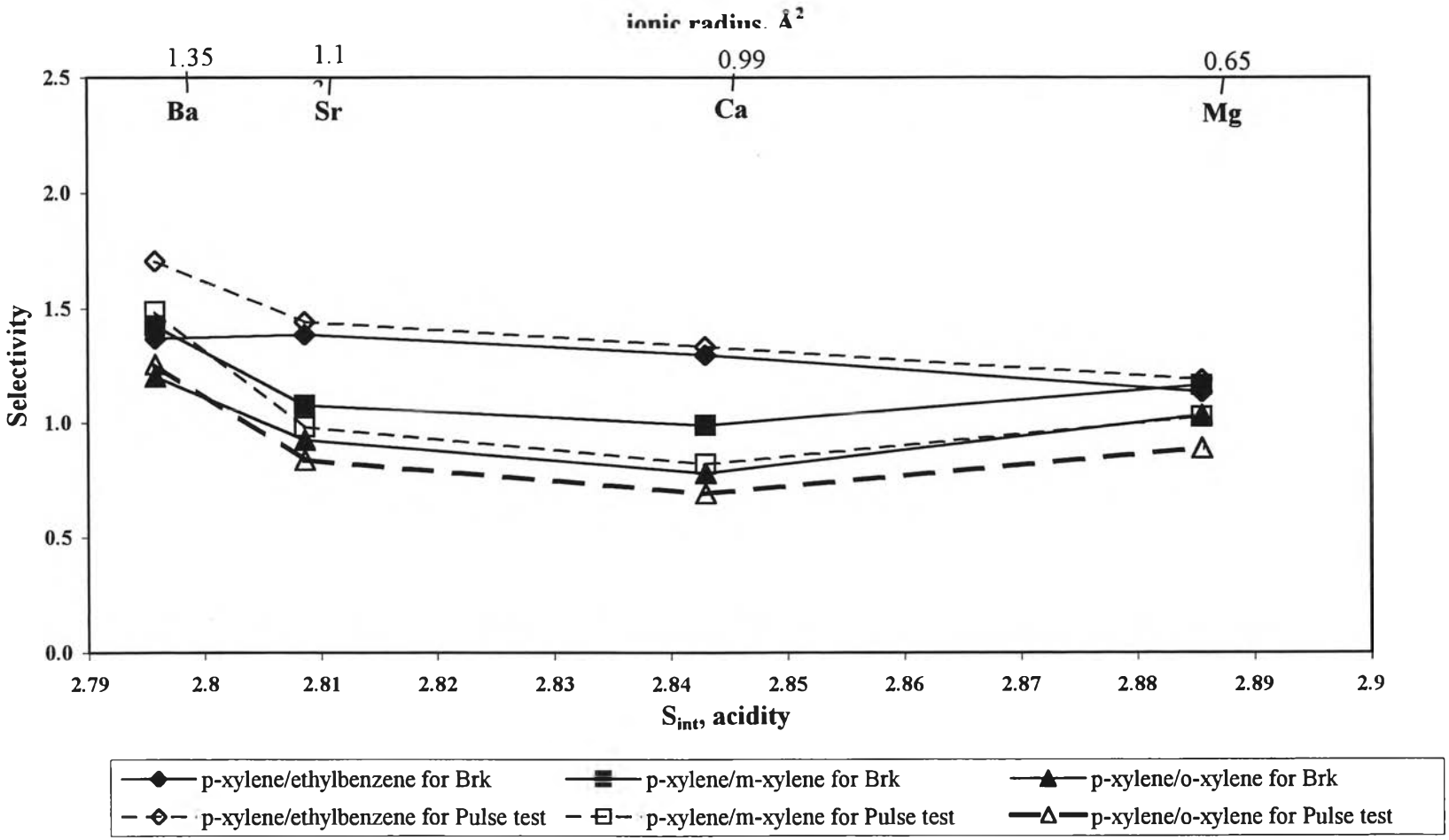

Figure 4.33 Comparison of p-xylene selectivity calculated from the Breakthrough and Pulse Test experiments for Y zeolite.